JOURNAL OF GEOPHYSICAL RESEARCH, VOL. 108, NO. B3, 2160, doi:10.1029/2002JB002015, 2003

Fossil hot spot-ridge interaction in the Musicians Seamount Province: Geophysical investigations of hot spot volcanism at volcanic elongated ridges

H. Kopp, C. Kopp, J. Phipps Morgan, E. R. Flueh, and W. Weinrebe
GEOMAR Research Center for Marine Geosciences, Kiel, Germany

W. J. Morgan
Department of Geosciences, Princeton University, Princeton, New Jersey, USA

Received 6 June 2002; revised 26 September 2002; accepted 25 November 2002; published 19 March 2003.

[1] The Musicians Seamount Province is a group of volcanic elongated ridges (VERs) and single seamounts located north of the Hawaiian Chain. A 327° trending seamount chain defines the western part of the province and has been interpreted as the expression of a Cretaceous hot spot beneath the northward moving Pacific Plate. To the east, elongated E-W striking ridges dominate the morphology. In 1999, wide-angle seismic data were collected across two 400 km long VERs. We present tomographic images of the volcanic edifices, which indicate that crustal thickening occurs in oceanic layer 2 rather than in layer 3. This extrusive style of volcanism appears to strongly contrast with the formation processes of aseismic ridges, where crustal thickening is mostly accommodated by intrusive underplating. High-resolution bathymetry was also collected, which yields a detailed image of the morphology of the VERs. From the occurrence of flat-top guyots and from the unique geomorphologic setting, two independent age constraints for the Pacific crust during the Cretaceous "quiet" zone are obtained, allowing a tectonic reconstruction for the formation of the Musicians VERs. Hot spot-ridge interaction leads to asthenosphere channeling from the plume to the nearby spreading center over a maximum distance of 400 km. The Musicians VERs were formed by mainly extrusive volcanism on top of this melt-generating channel. The proposed formation model may be applicable to a number of observed volcanic ridges in the Pacific, including the Tuamotu Isles, the eastern portion of the Foundation chain, and the western termination of the Salas y Gomez seamount chain. *INDEX TERMS:* 3025 Marine Geology and Geophysics: Marine seismics (0935); 7220 Seismology: Oceanic crust; 8180 Tectonophysics: Tomography; 8434 Volcanology: Magma migration; 9355 Information Related to Geographic Region: Pacific Ocean; *KEYWORDS:* volcanic elongated ridges, hotspot-ridge interaction, seismic tomography

Citation: Kopp, H., C. Kopp, J. Phipps Morgan, E. R. Flueh, W. Weinrebe, and W. J. Morgan, Fossil hot spot-ridge interaction in the Musicians Seamount Province: Geophysical investigations of hot spot volcanism at volcanic elongated ridges, *J. Geophys. Res.*, *108*(B3), 2160, doi:10.1029/2002JB002015, 2003.

1. Introduction

[2] Global satellite altimetry data have sufficient resolution to see wide variations in the types of volcanic structures found on oceanic seafloor. A large fraction of this volcanism has been emplaced near oceanic spreading centers; different models of hot spot-ridge interaction have been proposed to explain its origin in terms of this observation. V-shaped ridges or seamount chains, with "type examples" found at the Reykjanes Ridge south of Iceland and the SE Indian Ridge, are understood to be produced by fixed or moving melt anomalies on a rise axis [*Vogt*, 1971; *Johnson and Vogt*, 1973] or the propagation of rift segments [*Hey and Vogt*, 1977; *Sempere et al.*, 1997]. Broad continuous aseismic ridges are often observed where a major plume is centered on (or very close to) a spreading axis. The thickened crust produced by enhanced plume melting leaves trails on the spreading crust like the Cocos/Carnegie Ridge [*Lonsdale and Klitgord*, 1978] or the Ninetyeast Ridge [*Mahoney et al.*, 1983]. An additional model for the development of aseismic ridges has been proposed by *Morgan* [1978], who postulated a sublithospheric asthenosphere flow from an off-axis hot spot to a spreading center. The additional melt supply increases the volcanic production where the channel reaches the ridge axis and causes the formation of volcanic ridges, created at the spreading center, of order 2 km height, which display a distinct azimuth arising from differences between the absolute and relative plate motion. The significant new development in this

0148-0227/03/2002JB002015$09.00

hypothesis was that here the plume and spreading center can interact over a distance of up to several hundred kilometers. Isotope geochemical evidence of such long-distance interaction between plumes and ridges was subsequently found by a number of studies [e.g., *Verma et al.*, 1983; *Hanan et al.*, 1986; *Yu et al.*, 1997; *Kingsley and Schilling*, 1998; *Keller et al.*, 2000]. However, the azimuths of many aseismic ridges in the Atlantic as well as in the Pacific appear to differ significantly from those predicted by the *Morgan* [1978] model. Aseismic ridges between Clipperton and Galapagos FZ, so-called "cross-grain ridges" have been interpreted to be produced by the filling of tensional cracks in the lithosphere that are caused by the drag of mantle convective rolls [*Winterer and Sandwell*, 1987]. *Searle et al.* [1995] and *Binard et al.* [1996] describe morphologically similar ridges west of the Easter Microplate, which they also interpret to be caused by lithospheric tension but in this case, due to thermal, tectonic, or volcanic load processes. For the formation of the Pukapuka ridges in the central Pacific, *Sandwell et al.* [1995] propose a diffuse extension model which they relate to slab-pull forces acting parallel to the strike of the East Pacific Rise.

[3] In the last decades, several near-axis topographic lineaments and seamount chains within a range of 0–200 km distance to the Mid-Atlantic Ridge (MAR) or East Pacific Rise (EPR) have been described with orientations that likewise cannot be explained by either absolute or relative plate movement. *Small* [1995] suggests that a hot spot may be incrementally attracted by the center of an approaching spreading segment producing oblique volcanic trails as observed, e.g., at Hollister Ridge, located obliquely between the EPR and the Louisville hot spot track. Different from *Morgan*'s [1978] scenario, Small suggests the deflected plume channel erupts on the ridge flanks and only in the latest stage on the ridge axis, where the melt is spread along the axis terminating the volcanic trail. From geochemical studies, *Geli et al.* [1998] and *Vlastelic et al.* [1998] show evidence that excludes a contribution of the Louisville hot spot to Hollister Ridge. They relate the volcanism to intraplate deformation processes.

[4] The ridge trends observed by *Schouten et al.* [1987] and *Clague et al.* [2000] near the EPR and MAR again fit perfectly to the trend predicted by Morgan's vector diagrams, although the morphology of the ridges seems to exclude hot spot influence. The axis-parallel motion component of the hot spot is replaced here by a subaxis asthenosphere flow that equals the motion of the hot spot frame (but not a certain hot spot) with respect to the ridge and the authors interpret the structures to be generated by the migration of asthenosphere-entrained volcanic segments along the ridge. One of the most prominent examples for the off-axis formation of volcanic ridges due to hot spot-ridge interaction is the eastern tip of the Foundation Seamount chain [*O'Connor et al.*, 1998]. Here, the production of individual seamounts produced by the Foundation hot spot switches to elongated ridges as the Pacific-Antarctic Ridge (PAR) approaches the hot spot [*Maia et al.*, 2000]. The hot spot-ridge interaction zone extends along the easternmost 400 km of the Foundation chain [*Maia and Arkani-Hamed*, 2002].

[5] Most studies on volcanic ridges are based on hydroacoustic and gravimetric measurements. Seismic investigations revealing deep crustal structures of aseismic ridges have recently been conducted at the Ninetyeast Ridge [*Grevemeyer et al.*, 2001], Cocos Ridge [*Walther*, 2003], Carnegie Ridge [*Flueh et al.*, 2001], Nazca Ridge [*Bialas et al.*, 2000], and Faroe-Iceland Ridge [*Staples et al.*, 1997]. These ridges are formed at spreading centers interacting with a near or on-axis hot spot and are regarded as "pure" hot spot tracks or aseismic ridges.

[6] The Musicians seamount region (Figure 1), the target of this study, is characterized by a number of roughly W-E trending ridges whose origin is still under discussion. The ridges are slightly oblique to the former relative plate motion, yet also clearly do not follow the trend of the absolute Pacific plate movement. *Epp* [1978, 1984] proposed that the ridges were created by flow of hot spot magma into weak transform faults paralleling major fracture zones. This interpretation was reinforced in a tectonic reconstruction for the Pacific and Farallon Plate evolution around 90 Ma by *Sager and Pringle* [1987]. They argue that a change in spreading direction might have induced extension along fracture zones, where magma ascended to the surface. The Musicians elongated ridges are situated west of the former Pacific-Farallon spreading center position and do not extend beyond the trail of the Euterpe hot spot to the west (so named after the muse of musicians in Greek mythology), suggesting that they might be a direct expression of plume-ridge interaction. We propose that the ridges were formed by off-axis volcanism on top of an asthenospheric channel extending from the hot spot to the Pacific-Farallon spreading center, as this hypothesis appears to explain the observed features. We use new seismic wide-angle and swath bathymetric data to investigate the impact of this kind of volcanism on the oceanic crustal structure and morphology in this area and also suggest a revision to Mesozoic Pacific plate motions in the Musicians province based on two independent geomorphologic observations.

2. Tectonic Setting

[7] The Musicians seamounts are located several hundred kilometers northwest of the Hawaiian chain (Figure 1). They are separated into a northern and a southern volcanic province by the Murray fracture zone. Seafloor mapping based on satellite altimetry [*Sandwell and Smith*, 1997] reveals several volcanic elongated ridges (VERs), which contain isolated volcanic summits along their crests. The lateral extent of the ridges increases southward in the northern and southern provinces, respectively (Figure 1), from less than 100 km to more than 400 km length. Two of the most prominent ridges, the northern Italian Ridge and the southern Bach Ridge (Figure 1), both trending in a E-W direction nearly parallel to the pronounced fracture zone in their vicinity, are the focus of this study. Their seamounts are found in variable water depths of 2.2 to 5.1 km (Figure 2). The Murray Fracture Zone, which crosses the Musicians Province, is ~130 km wide (Figure 3) and displays a ridge-and-trough morphology. As no discernable offset of the Musician seamounts across the fracture zone is observed, several authors [*Freedman and Parsons*, 1986; *Sager and Pringle*, 1987] have suggested that the Musicians were emplaced after transform fault activity ceased.

[8] A linear, 327° trending volcanic chain defines the western boundary of the Musicians province, where the

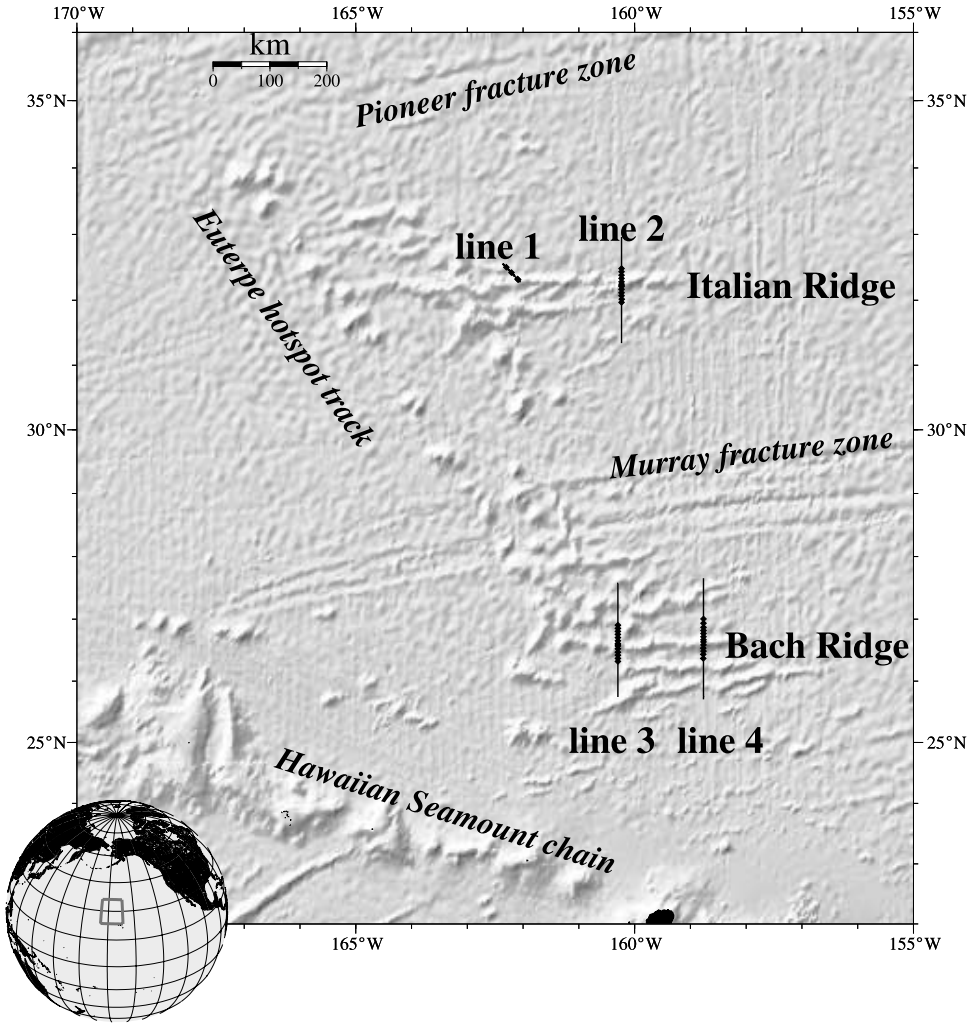

Figure 1. Location map of the Musician seamounts north of the Hawaiian Chain. The 327° trending Cretaceous Euterpe hot spot track marks the western boundary of the volcanic province. No evidence for volcanism is found north of the Pioneer fracture zone. The Musician volcanic elongated ridges (VERs) trend in an E-W direction. The Murray fracture zone splits the study area into northern and southern subregions with similar VER behavior observed in each. The increasing length of the ridges from north to south in the two volcanic areas is a unique feature of this province. This, and the abrupt termination of the ridges at the hot spot track, are both explained by hot spot-ridge interaction forming a partially melting asthenospheric flow channel between the Euterpe plume and the fossil Pacific-Farallon spreading center to the east. Geophysical investigations were conducted along the northern Italian Ridge and the southern Bach ridge. Wide-angle seismic data were acquired along four profiles and are complemented by high-resolution bathymetric data.

elongated volcanic ridges are only recognized to the east and distinctly terminate at the Cretaceous Euterpe hot spot track. The (now extinct) Euterpe center would be at 10°S, 124°W. Ar-Ar age datings from *Pringle* [1992] confirm the hot spot hypothesis for this chain and reveal ages between 96 Ma in the north and 82 Ma in the south with a progression rate of 57 km Myr^{-1}, which makes it one of the oldest hot spot tracks on the Pacific plate. The Euterpe hot spot track terminates at the Pioneer Fracture Zone (line A in Figure 3), which parallels the Mendocino Fracture Zone to the north (Figure 3). Prior to 96 Ma, the hot spot trail altered the Farallon plate north of the large offset (800–1000 km) Mendocino transform fault before the northwestward moving Pacific plate moved over the hot spot. Today, all hot spot traces on the Farallon plate have vanished since this portion of the plate has been subducted beneath North America [*Sager and Pringle*, 1987; *Pringle*, 1993]. An additional feature of this volcanic chain which supports its interpretation as a hot spot track is its parallelity to within a few degrees to the northernmost tip of the Emperor chain (from Detroit seamount (81 Ma) to Meiji seamount (age unknown) [*Keller et al.*, 1995]), which is of comparable age to the Euterpe chain and thus records the same absolute plate motion.

[9] The age of the underlying Pacific crust is not clear, as it formed during the Cretaceous "quiet zone" (~118–83 Ma) when the Earth's magnetic field did not reverse polarity. Extrapolation of the magnetic anomalies by *Müller et al.*

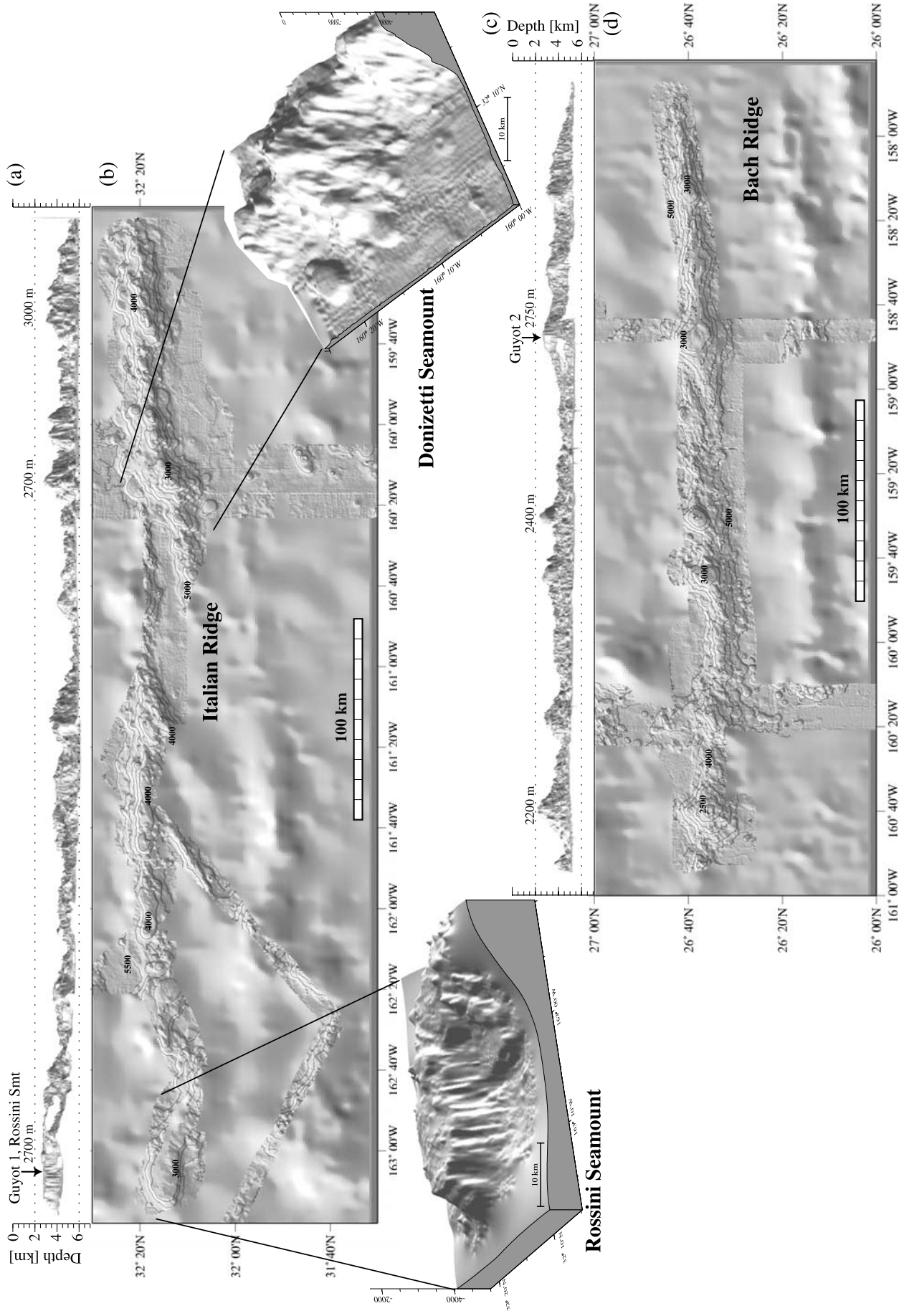
(a)
(b)
(c)
(d)
Depth [km]
Guyot 1, Rossini Smt
2700 m
3000 m
2700 m
2400 m
2200 m
Guyot 2
2750 m
Italian Ridge
Donizetti Seamount
Rossini Seamount
Bach Ridge
100 km
10 km

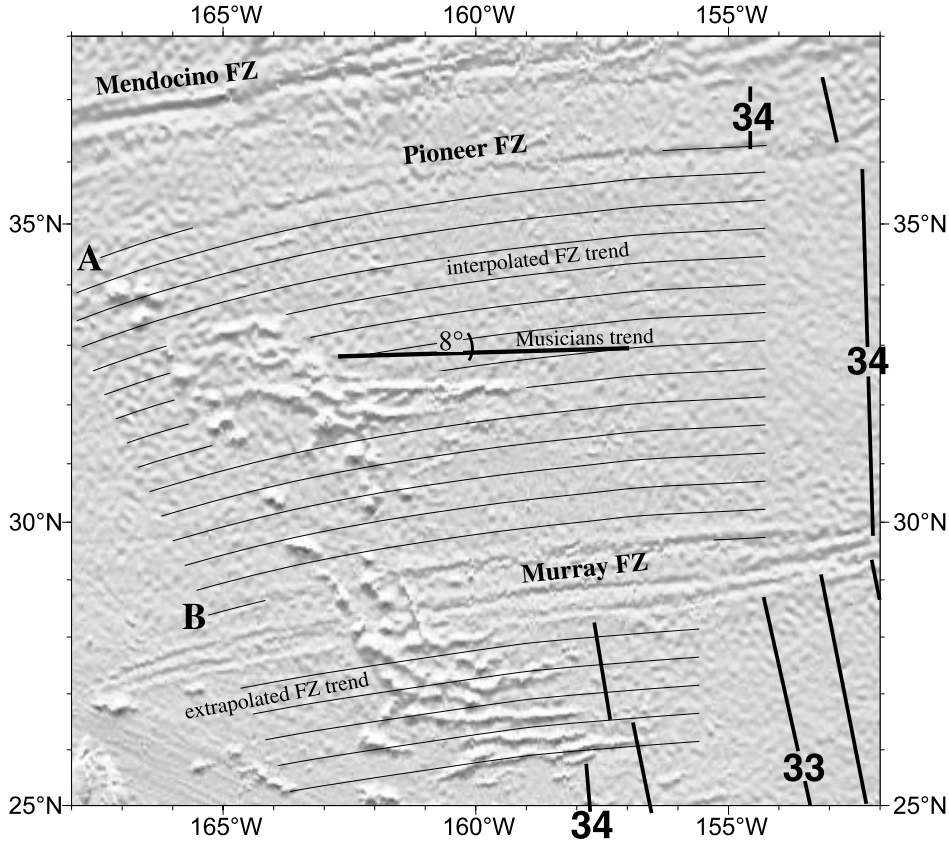

Figure 3. Interpolated fracture zone trends between Pioneer and Murray Fracture zones (A and B) deviate by ~8° from the trend of the Musician VERs. Thus their origin cannot be directly associated with that of these fracture zones. Thick black lines indicate magnetic anomalies before the Cretaceous quiet zone. M33 and M34 correspond to ~75 Ma and 84 Ma, respectively [*Atwater and Severinghaus*, 1989].

[1997] yields crustal ages beneath the Musician Seamount Province of ~110 Ma, which would imply a period of extremely rapid spreading of ~13 cm yr^{-1} between 120 and 110 Ma, followed by slower spreading at only 1/3 of the rapid opening rate. This would imply that the Musicians were formed on ~15 Myr old crust. *Freedman and Parsons* [1986] propose a much younger age of the seafloor at the time of the seamount emplacement. Their investigations on the crustal elastic thickness yield a lithospheric age of <5 Ma at the time the Musicians were formed [*Freedman and Parsons*, 1986].

3. Data Acquisition and Processing

[10] The HULA field campaign conducted with the R/V *Sonne* in 1999 [*Flueh et al.*, 1999] investigated two of the most prominent Musicians ridges in detail. To classify their type of volcanism with reference to other marine volcanic ridges and examine the formation of these ridges, the northern Italian Ridge and the southern Bach Ridge were mapped with wide-angle seismic, magnetic (W. W. Sager et al., manuscript in preparation, 2002), and hydroacoustic measurements. Geochemical analyses and age dating of several dredge samples along the ridges are still in progress. Here, we present the seismic wide-angle data that were collected along three lines across the ridges supplemented by high-resolution swath bathymetric images of the entire length of Italian and Bach Ridge. The three longer seismic lines (Figure 1) are between 180 and 220 km long and on each of them, 12–14 ocean bottom hydrophones (OBH) were placed in the central part of the lines with a mean spacing of 4 km. Two Bolt air guns with a total volume of 64 I were used as the seismic source. With a shot interval of 60 s and a speed of 4 kt, a shot spacing of

Figure 2. (opposite) High-resolution bathymetric images of the two most prominent ridges of the Musician volcanic province. The swath data is underlain by predicted bathymetry from satellite altimetry data [*Sandwell and Smith*, 1997] (Figures 2b and 2d). The coherent ridges, up to 400 km long, are characterized by distinct volcanic cones and en echelon segments. In the side view displayed in Figures 2a and 2c, at least one guyot along Italian Ridge and Bach Ridge, respectively, is recognized. Donizetti Seamount and flat-topped Rossini Seamount, both located along the Italian Ridge, are enlarged. From the height of the erosional flat tops the distance of the guyots to the Pacific-Farallon spreading ridge at the time of their formation may be inferred, yielding an independent constraint for the age of the Pacific crust at the time of their formation. See text for further details.

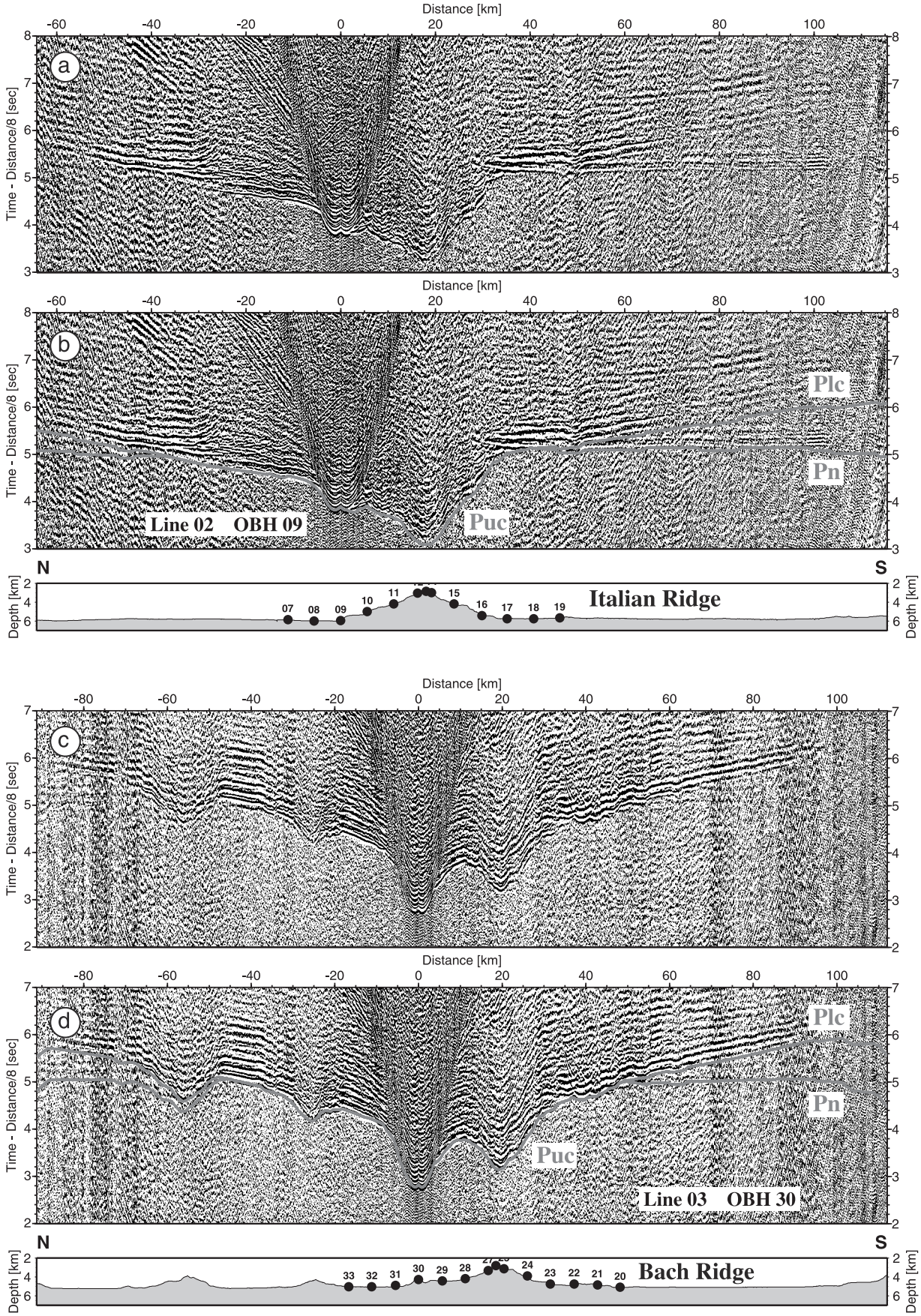
Distance [km]
-60 -40 -20 0 20 40 60 80 100
a
b
Time - Distance/8 [sec]
Plc
Pn
Puc
Line 02 OBH 09
N
S
Depth [km]
07 08 09 10 11 15 16 17 18 19
Italian Ridge
-80 -60 -40 -20 0 20 40 60 80 100
c
d
Line 03 OBH 30
33 32 31 30 29 28 24 23 22 21 20
Bach Ridge

~120 m was achieved. The data were recorded after antialias filtering at a sampling rate of 5 ms. In contrast to a well-tuned air gun array, the two large guns produced a rather oscillating signal. However, the seismic signal was able to be significantly improved by a processing sequence adapted to the special data characteristics. We applied a time-gated Wiener deconvolution with a gate length of 2 s. Filtering of wide-angle seismic records has to be done carefully, as the frequency content can differ not only with travel time but also laterally with the travel path, whereas attenuation in the water column is neglectable. To account for these difficulties we applied a static water depth correction of the traces prior to an offset- and time-dependent frequency filter.

[11] High-resolution hydroacoustic seafloor mapping was conducted along the Italian Ridge and the Bach Ridge (Figure 2) using RV SONNE's onboard Hydrosweep multibeam system [*Grant and Schreiber*, 1990] with a 90° beam angle resulting in a swath width of 2 times the water depth. Subsequent processing of each sweep was carried out using the mbsystem [*Caress and Chayes*, 1996] and GMT [*Wessel and Smith*, 1991] software tools. Sound velocities were also constrained by CTD measurements [*Flueh et al.*, 1999].

4. Morphology of the Musicians Volcanic Elongated Ridges (VERs)

[12] Global satellite altimetry data [*Sandwell and Smith*, 1997] suggest the Musicians consist of mostly E-W trending, nearly continuous ridges. The new bathymetric data reveals more details of the ridges' morphology. In Figure 2, the high-resolution swath mapping data of Italian Ridge and Bach Ridge overlay the "predicted bathymetry" [*Sandwell and Smith*, 1997]. The general 90° trend is overlain by oblique en echelon segments trending ~84°, most obvious at the Italian Ridge in Figure 2b. The ridges have a mean height of 2000 m and are dominated by prominent volcanoes emerging to a maximum height of 3500 m above the surrounding seafloor with a spacing from 30 km to 80 km (e.g., Donizetti Seamount in Figure 2). Despite these dominating volcanoes, the structure is significantly different from the Vance, President Jackson and Taney near-ridge seamounts in the northeastern Pacific described by *Clague et al.* [2000], which consist exclusively of circular, isolated seamounts on a linear chain. The overall morphology of the Musicians is rather rough. Volcanism is fairly focused on discrete ridges, similar to the Pukapuka ridges in the central Pacific [*Sandwell et al.*, 1995], but there are also several small volcanic cones with diameters between of 3 and 6 km on the nearby flat seafloor (Figure 2). Some examples are found adjacent to the base of Donizetti seamount as visible in the enlarged section of Figure 2. Diffuse lithospheric extension has been proposed as the origin process for the Pukapuka ridges [*Sandwell et al.*, 1995]; however, there the investigated ridges are elongated in the direction of present absolute plate motion, which was clearly not the case during the formation of the Musician VERs. Nevertheless, there are several morphological features of the Musicians which show a striking similarity to the Pukapuka ridges, including their commonly very linear trend and the oftentimes elongated volcanic edifices (e.g., Rossini and Donizetti seamounts in Figure 2) atop the ridge segments. For the Pukapuka ridges this morphology has been interpreted to be indicative of an origin as tension cracks [*Lynch*, 2000], which may also apply to the Musicians ridge segments.

[13] The swath data give clear evidence for at least one major flat-topped seamount on Italian and on Bach Ridge, respectively. Guyot 1 (Rossini seamount, enlarged in Figure 2) at the western tip of Italian Ridge emerges from the surrounding seafloor by 2950 m. It is elongated in the ESE direction, its flat top measuring 11 km × 3 km. Guyot 2 is located on the eastern part of Bach Ridge with a height of 2650 m above seafloor level (Figure 2c). The circular flat summit, 3 km in diameter, is part of an ENE elongated ridge segment. Both Guyot summits reach water depths of 2700 m. Nevertheless, they display different relative heights resulting from different depths of the surrounding seafloor, as the southern part of the Musicians is 300 m shallower due to the younger lithosphere south of the Murray FZ and the influence of the nearby Hawaiian swell. The highest volcanoes on the two investigated ridges are labeled with water depths in Figures 2a and 2c. They have noneroded tops and, particularly on Bach Ridge, they exceed the height of the Guyots by some hundred meters.

[14] The relation of the Musicians ridges to the adjacent fracture zones is enigmatic. Because of Cretaceous plate reorganizations, the major North Pacific fracture zones show a complex pattern with multiple changes from single fractures to broad scattered relay zones around the Musicians. Nevertheless, the interpolation of the Pioneer and Murray fracture zones as done from the satellite altimetry data set in Figure 3 shows that their trends around the northern Musicians region correspond perfectly to each other: A simple shift of the Pioneer FZ trend (line A in Figure 3) matches the northernmost trace of the Murray FZ (line B). The orientation of the southern Musicians ridges is roughly parallel to the Murray FZ, but from SE to NW, the fractures are getting increasingly oblique and the Musicians ridges do not follow this trend. Instead, their orientation remains constant (89°) in the whole area, regardless of the fracture trend. As seen in Figure 3, at the northern Italian Ridge the trend deviation is ~8°.

5. Tomographic Inversion Method

[15] The seismic sections (examples presented in Figures 4 and 5) show a uniform data quality on the three seismic lines. Most of the stations have clear recordings in the entire

Figure 4. (opposite) Seismic wide-angle sections for (a and b) OBH 09 of line 02 and (c and d) OBH 30 of line 03. Figures 4b and 4d illustrate the calculated travel times on top of the seismic data shown in Figures 4a and 4c. Clear phases from the lower crust (*Plc*) and mantle (*Pn*) to offsets reaching 100 km are observed on a number of stations and are influenced by the pronounced morphology of the volcanic province. The tomographic inversion applied to the data employs primary as well as secondary arrivals to include a maximum of travel time information. Successive inversion of different offset ranges using a top-to-bottom approach recovered the crustal velocities.

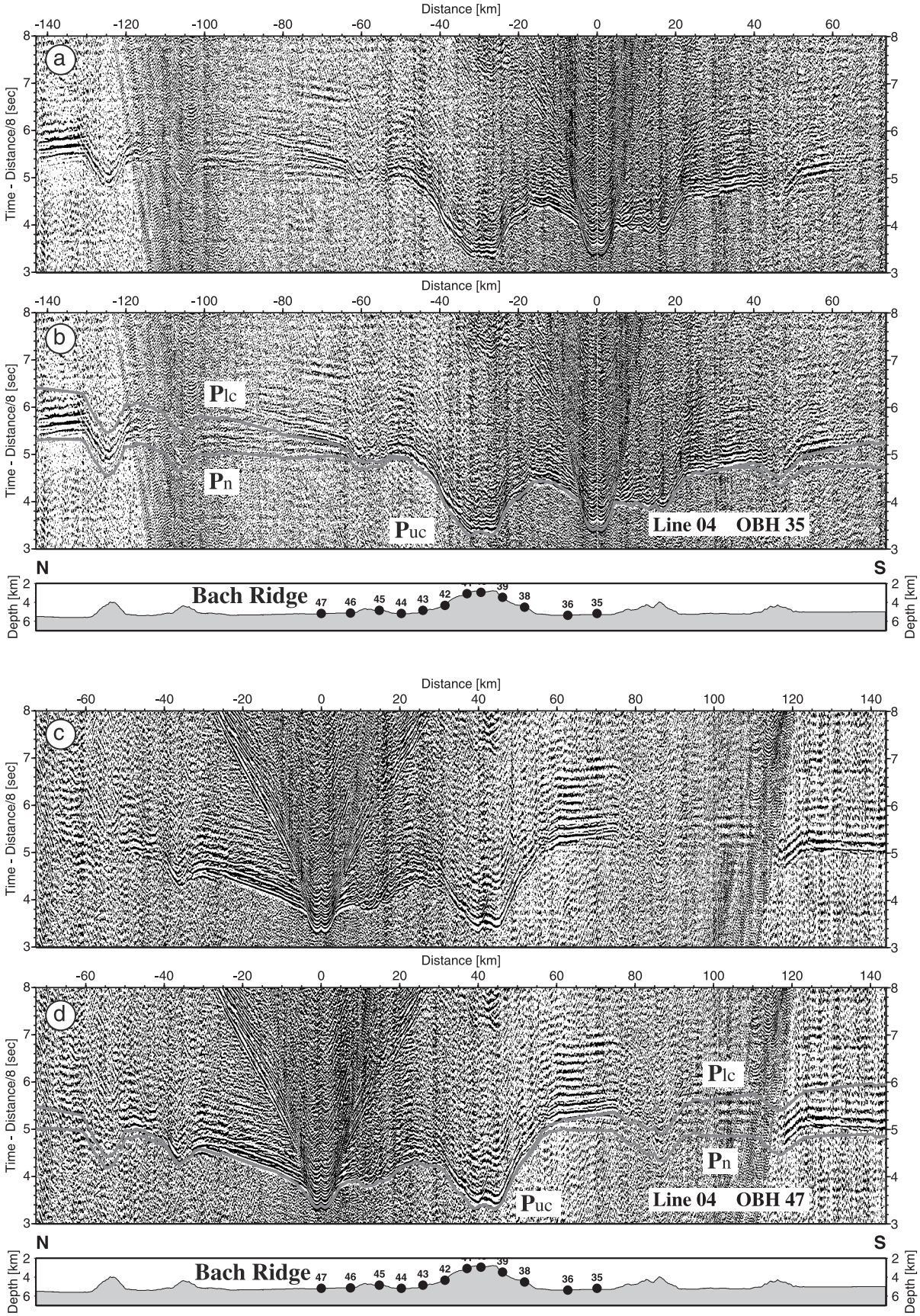

Figure 5. Seismic wide-angle sections for OBH 35 and OBH 47 of line 04 across Bach Ridge. See Figure 4 caption for display information; 12 to 14 instruments were deployed on each profile. See text for further details.

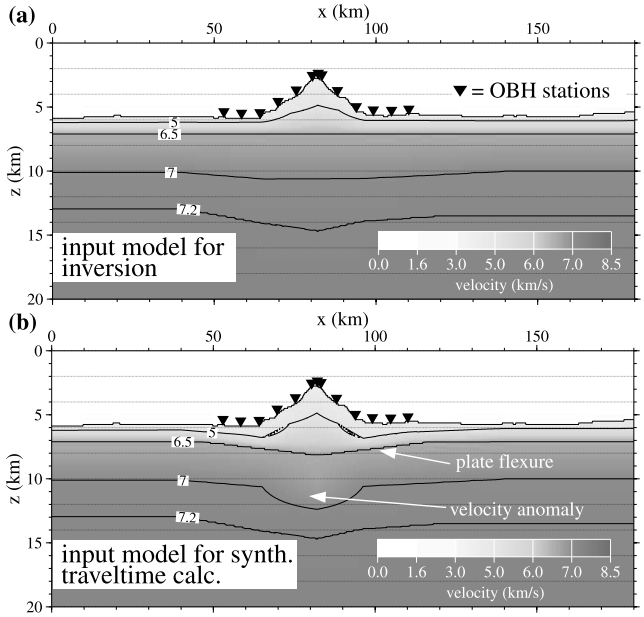

Figure 6. (a) Input starting model for the inversion using crustal arrivals. Topographic information is included in the starting model, which assumes a standard oceanic crust. As mantle phases were omitted during this stage of the inversion, the model displays a crust of infinite thickness. (b) Model used as the input model for the synthetic travel time calculation and thus representing the desired inversion output. In contrast to the model in Figure 6a it displays flexural downbending of the crust centered beneath the volcanic edifice and a velocity anomaly in the lower crust.

shot-receiver offset range, up to the maximum offset of 140 km (e.g., OBH 35 and OBH 47 in Figure 5). Only in the central part of line 4, some stations display a lower signal-to-noise ratio attenuating phase coherency beyond 50–70 km offset. The seismic sections are strongly affected by the bathymetry of the ridges, which causes drastic changes in apparent velocities. However, the upper crustal refraction (*Puc*), lower crustal refraction (*Plc*) and mantle refraction (*Pn*) can be clearly differentiated on almost every station and reveal relatively smooth interval velocity structures across the ridges.

[16] We used the FAST tomography code [*Zelt and Barton*, 1998] for our computations. This method is a first-arrival tomography utilizing the ''regularized inversion'' on a uniform velocity grid. The velocity models were defined with a grid size of 2 km in x and 0.5 km in z direction. In total, more than 8000 first-arrival travel time picks per line were used for the inversions. The first arrivals up to ~25 km offset are related to upper crustal refractions (phase *Puc* in Figures 4 and 5) and merge with only gradual velocity changes into the lower crustal refractions *Plc*. Together with the mantle reflection *PmP* these extend to large offsets of up to 100 km with high amplitudes, which is a distinct phenomenon of this data set (e.g., OBH 09 and OBH 30 in Figure 4). Between 40 and 100 km, the lower crustal refractions *Plc* are ''covered'' as second arrivals behind the first-arrival mantle refraction *Pn*. A standard inversion of these travel times using a first arrival tomography scheme would take primarily the upper crustal and the mantle arrivals into account. There are two problems with this approach: First, with this data set nearly 1/3 of the travel time information would not be considered when omitting the second arrival refractions between 40 and 100 km offset (i.e., phase *Plc*), thus resulting in poorer resolution of the lower crust. Second, tomographic inversions of active seismic experiments often fail in reproducing reasonable upper mantle structures. The forward calculation technique used in the FAST code is capable of handling large velocity contrasts [*Hole and Zelt*, 1995], but a grid-based inversion generally must seek for a smooth solution to explain the observed travel times, which fails to resolve sharp velocity contrasts like the crust-mantle boundary.

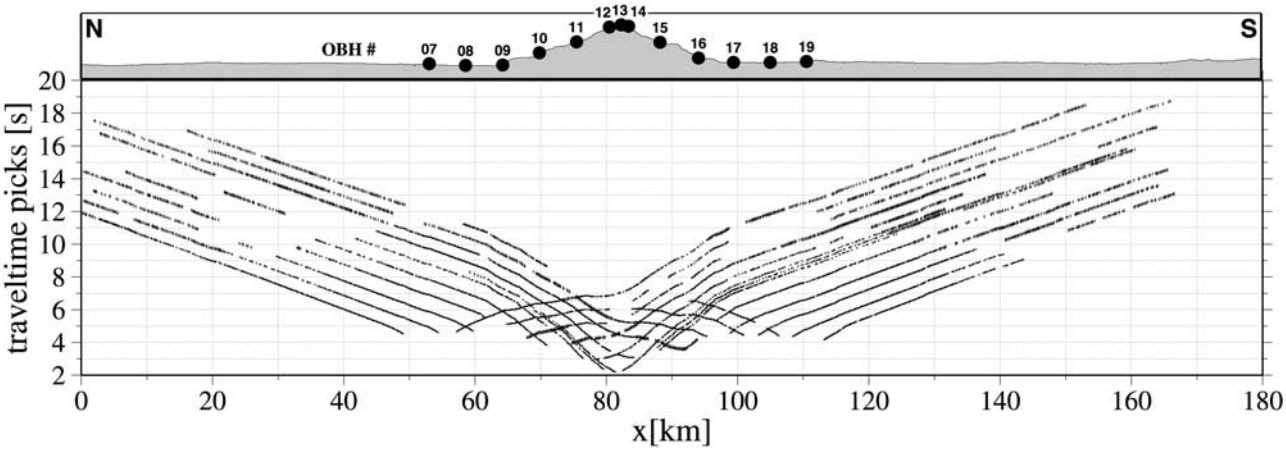

Figure 7. Synthetic travel time picks were generated using the source-receiver geometry and bathymetry of the experiment. Coverage of the travel time picks is identical to the real experiment. The synthetic data are used for resolution tests (discussed in text) to verify if the crustal characteristics of the test model displayed in Figure 6b may be retrieved with the experiment layout. The smooth input model for the synthetic resolution test is displayed in Figure 6a. Both models are used to image the crust and thus neglect any mantle phases.

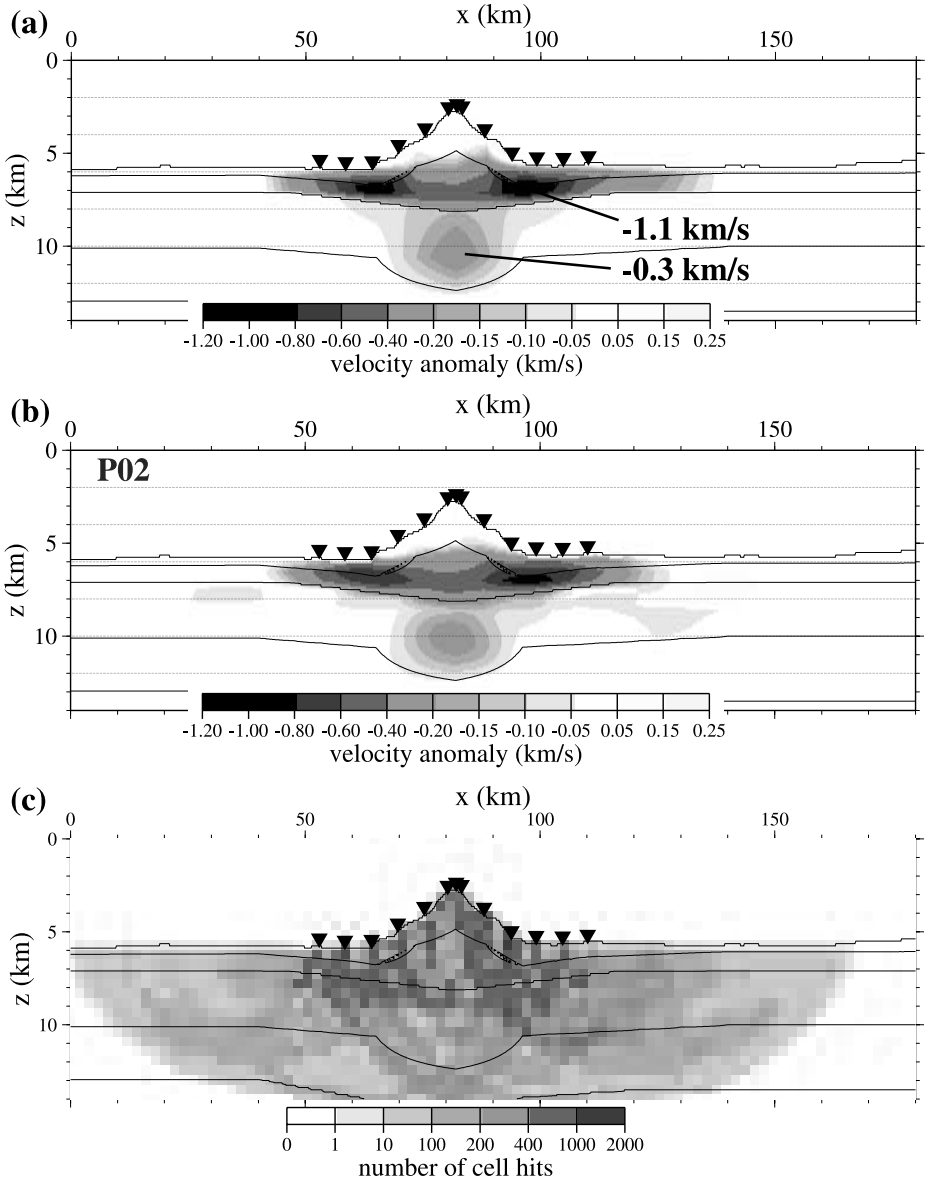

Figure 8. (a) Desired inversion velocity update, i.e., difference between the input models for the synthetic travel time calculation and for the inversion, respectively, as displayed in Figures 6a and 6b. The model difference is characterized by three velocity anomalies, which must be retrieved by the inversion process. The plate flexure causes two elongated anomalies of -1.1 km s^{-1}. A lower crustal anomaly of almost circular shape has an amplitude of -0.3 km s^{-1}. (b) Difference between the input model and the inversion result. All anomalies are clearly resolved in position, shape, and amplitude. (c) Ray coverage achieved for the inversion cells with a maximum coverage of 1000 hits per cell.

Furthermore, the requirement of a uniform ray coverage is violated by the special geometry of the *Pn* phases. To overcome these problems, the following approach was employed: In order to keep the starting model as simple as possible, we generated a normal oceanic crust velocity model with laterally constant $v(z)$ dependence below the seafloor, according to the "minimum 1-D model" of *Kissling et al.* [1994]. As a pure 1-D structure would be rather unrealistic at the volcanic dome, the model is adjusted to the known bathymetry and to a realistic 2-D structure at the central volcano as shown for line 2 in Figure 6. The approximate travel time fit of the model was achieved by forward ray tracing [*Zelt and Smith*, 1992], and computation of RMS misfits for different models was used to select the best starting model. The resolution of the computed inversion image was improved by using a "layer stripping" inversion method with three iterations. In the first step, only travel time picks with offsets up to 25 km were taken into account, yielding an image of the upper crust. Upper crustal velocities were held fixed in the next iterations. In a second step only offsets >25 km have been inverted with the aim of recovering lower crustal velocities. The rays through the lower crust are mostly represented by secondary arrivals behind the mantle refraction (*Pn*). Therefore the mantle

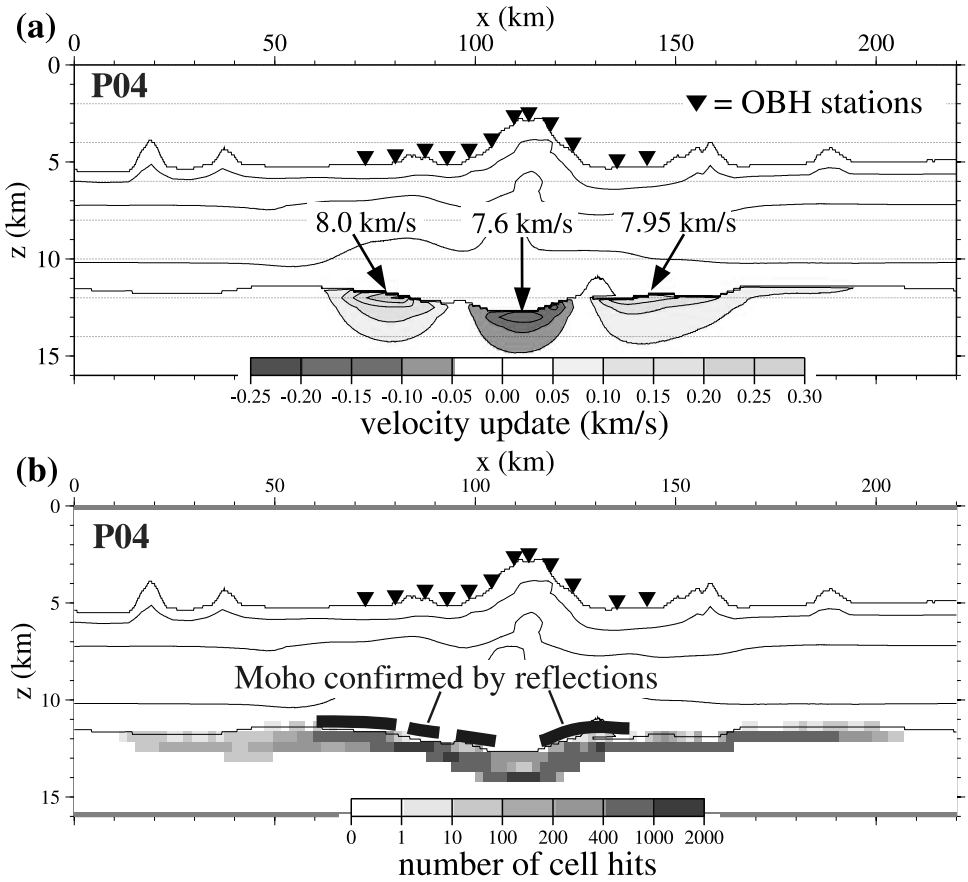

Figure 9. (a) Inversion of upper mantle velocities on line 4. The mantle refraction *Pn* was inverted while keeping the crustal information unchanged. (b) The velocity update. The position of the Moho is inferred from forward modeling of the mantle reflections and is kept fix during the mantle inversion. Decreased mantle velocities underneath the central volcano were always retrieved for different starting velocities and Moho depths. The ray mantle coverage achieved during the inversion is also displayed.

phases have been omitted in this step. Consequently, also the mantle had to be omitted in the starting model, resulting in a crust of infinite thickness as shown in Figure 6. The last step then consisted of an inversion for mantle velocities. Forward ray tracing of the mantle phases *PmP* and *Pn* was used to define the depth of the Moho, which during a subsequent inversion of the mantle refraction *Pn* was held fixed to recover the upper mantle velocities.

6. Resolution Tests

[17] Prior to the final inversion of the data, a number of synthetic tests were conducted in order to determine the optimal inversion parameters and reliable resolution of each inversion. Although a few kilometers is probably a good estimate for the length scales of the smallest resolved anomalies, the target of these investigations is to unravel larger structures, particularly those giving insight to the mechanisms that have formed the Musicians ridges. To discriminate between possible formation scenarios, it is key to explore the relation of upper to lower crustal structures: If the ridges were formed by tectonic uplift in a compressional regime, the crustal thickness would be unchanged and the Moho would follow the seafloor trend, largely plutonic volcanic formation would thicken the lower crust; while largely extrusive volcanic formation would lead to a thickening of the upper crust with associated flexural downbending of the lithosphere. Additionally, there may be underplating below the seismic Moho with velocities between crust and mantle values. A simulation of plate flexure and velocity anomalies in the lower crust was investigated using synthetic tests. In each resolution test we ask if the inversion method is capable of resolving the upper and lower crustal structure and if the data is sensitive to the presence of a plate flexure. Possible plate flexure does not necessarily yield a characteristic morphologic signature, since the resulting moat could be filled by volcanoclastic material. However, our tomographic inversion would be able to resolve the lower seismic velocities of such moat infill. The velocity model in Figure 6b was used to calculate synthetic travel times with a source-receiver geometry and coverage of travel time picks identical to the real experiment (Figure 7). Additionally, synthetic noise was added. Using these synthetic data and a smooth input model for an inversion should retrieve the simulated crustal characteristics. Random noise was added to the calculated synthetic travel times with a standard deviation equal to the estimated error of the travel time picks (between 0.03 s at near offsets and 0.12 s at the far offset traces). The general velocity structure of the test model in Figure 6b is taken with minor

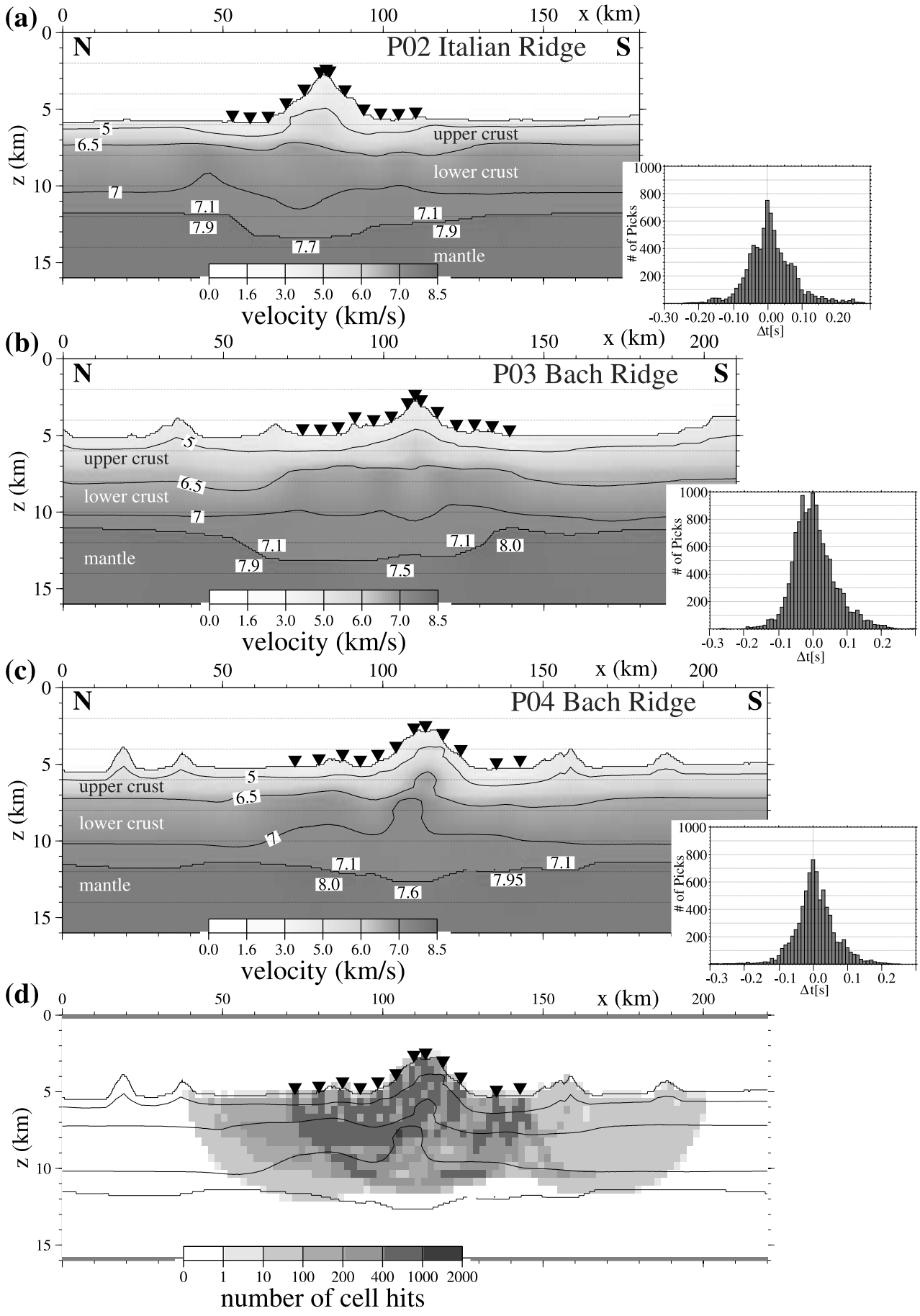
(a)
N
P02 Italian Ridge
S
x (km)
z (km)
upper crust
lower crust
mantle
5
6.5
7
7.1
7.9
7.7
velocity (km/s)
# of Picks
Δt[s]
(b)
P03 Bach Ridge
8.0
7.5
(c)
P04 Bach Ridge
7.6
7.95
(d)
number of cell hits

simplifications from line 2, including plate flexure and lower crustal velocity anomaly, which are to be found from the inversion. The smooth input model for the synthetic resolution test is displayed in Figure 6a, without plate flexure and without any lower crustal velocity anomaly. In both models, the lower crustal velocities are extrapolated to 20 km depth and mantle phases are neglected as described earlier. Figure 8a displays the difference between the input model for the synthetic travel time calculation and the starting model for the inversion, respectively (as shown in Figures 6a and 6b). The model difference consists of three velocity anomalies, which are to be retrieved during the inversion. Plate flexure causes two elongated anomalies of -1.1 km s^{-1}, while the lower crustal anomaly is almost circular in shape with an amplitude of -0.3 km s^{-1}. The difference between the input model and the final model is displayed in Figure 8b. The final model was gained after a separate inversion of the upper and the lower crust (with 3 iterations for each domain). All anomalies are clearly resolved in position, shape, and amplitude. The final model's upper crustal anomalies are only slightly lower in amplitude (compared to Figure 8a) and also are terminated where the coverage decreases away from the OBH stations. There are artifacts around 30 and 130 km, but with only small amplitudes. The ray coverage for the inversion cells of line 2 is shown in Figure 8c, where a maximum coverage of up to 1000 hits per cell is achieved. Thus the geometry used during the field campaign allows to resolve crustal structures beneath the positions of the OBH stations and with some restrictions also in the line periphery.

7. Crustal and Upper Mantle Structure

[18] The inversion parameters as well as the input model used for the synthetic inversion tests were applied to the real data. The calculated travel times obtained from the final inversions are plotted on the seismic sections in Figures 4c, 4d, 5c, and 5d. Except for minor fluctuations, a good fit could be achieved between model and observed travel time. The inversion scheme comprises a crustal tomographic inversion and a complementary subsequent upper mantle inversion (Figure 9) which is not allowed to alter the crustal tomographic result.

[19] The final inversion models for the three major lines are presented in Figure 10, where the lowermost image shows a representative ray coverage (P04) achieved during the inversion process. Sediment cover is not recognized at either VER. While the upper and lower crust as well as the upper mantle is clearly resolved along all three profiles, the internal structures vary between the lines. Figure 10a displays the crustal model for line 2, where a downbending of the upper crust is discernable from the trend of the velocity contours and the Moho. The downflexing results in a moat structure adjacent to the central volcano. It cannot be recognized in the morphology, because it is filled with volcanic debris as inferred from its low (<3.5 km s^{-1}) seismic velocities. A similar flexural structure is also recognized along profile 4 (Figure 10c). This down flexing of the oceanic crust results from top loading of the volcanic edifice. The thickened upper crust along these lines implies a ridge evolution dominated by extrusive volcanism above preexisting oceanic crust. Velocities increase within the upper portion of the crust from 4.4 to 6.5 km s^{-1} corresponding to a velocity gradient of 0.9 s^{-1}. The third line (Figure 10b) shows a rather complex structure, which may be anticipated from the presence of numerous smaller volcanoes around the central volcano, which is not as large and prominent as along the other two lines. No clear flexural bending or moat structure in the upper crust is resolved. It seems clear, however, that the upper crust is characterized by an increased thickness away from the central volcano (Figure 10b), which is not the case along the other two lines. The volcanic edifices show increasing velocities with depth (up to 5.7 km s^{-1} for the large central volcanoes on profiles 2 and 3 and up to 6.2 km s^{-1} on profile 4, respectively), evident from the upward deflection of the upper crust velocity contours, following seafloor relief. The lower crust is characterized by a reduced velocity gradient of 0.13 s^{-1}, with velocities increasing to 7.1 km s^{-1}. Along profile 3, the lower crust displays some thickening, as along the other two lines, however, here the zone of thickening is broader than on profiles 2 and 4, where a deflection of the Moho is mainly restricted to the area underneath the central volcano (Figures 10a and 10c). On the basis of the inversion models an extrusive dominated type of volcanism is inferred for the Musicians, though secondary intrusive processes may not be ruled out.

[20] Subsequent inversion of the mantle refraction (*Pn*) was conducted while keeping the crustal information unchanged. The resulting velocity correction is presented in Figure 9 for line 4. The thick lines in Figure 9b indicate the Moho deflections where constrained by mantle reflections during the forward modeling procedure. The resulting velocity perturbations show decreased mantle velocities underneath the central volcano, corresponding to inferences from the forward modeling. Tests with different starting velocities and different Moho depths yield the same result. The Moho reflections identified during the forward modeling process (bold lines in Figure 9) are restricted to the flanks of the thickened portion of the crust and cannot be identified in the central part where lowered velocities have been inferred. The bottom image displays the ray coverage during the mantle inversion, where no deep penetration is to be expected since the mantle refraction travels close to the crust-mantle boundary. Even though reduced mantle velocities are revealed in a small area underneath the ridge centers, underplating appears to be insignificant here. The seismic data do not show wide zones of reduced mantle velocities and supplementary reflections near the Moho reflection. These would be related to a layer of material underplated

Figure 10. (opposite) (a–c) Final inversion models for the three major profiles and corresponding residuals. Lines 02 and 04 display a flexural downbending of the crust. The thickened upper crust along all profiles is indicative of extrusive volcanism above the preexisting oceanic crust. The lower crust displays a decreased velocity gradient compared to the upper portion and a deflection of the Moho underneath the central volcano. Clear evidence for underplating is not observed on any of the lines. Residuals were computed using crustal phases. (d) Ray coverage along profile 04.

beneath the crust like has been found, e.g., at the Ninetyeast Ridge, Gran Canaria, and Hawaii [*Grevemeyer et al.*, 2001; *Ye et al.*, 1999; *Watts and ten Brink*, 1989].

[21] Figure 11 shows a global compilation of different hot spot related volcanic edifices with an identical scaling. All of these were located directly above a hot spot at the time of their formation and all of these show possible signs of underplating, though alternative models have also been proposed for Hawaii and Gran Canaria. For comparison, the Musicians, which are of much smaller size, are displayed at the bottom. Most of the larger volcanic edifices show indications of intrusive volcanism or underplating (Tenerife being the only exception). Extrusive processes without any indication for underplating seem to dominate in the evolution of the Musicians. Perhaps the different structure of the Musicians VERs results from their volcanoes not being formed on top of a hot spot, but rather between an off-axis plume and spreading center.

8. Inferences From Geomorphological Relations

[22] The inferred extrusive-type volcanism dominant during the formation of the Musicians seamounts is also supported by their rough morphology. The rugged topography implies that the ridges were created by a number of consecutive eruptions with a relatively low effusion rate over a long period of time. The narrow width of the ridges ($\sim$15 km) indicates an off-axis magma source, confined to a narrow constructional lineament. In particular the number of small volcanic cones between the ridges has in earlier papers been seen as an indication that the Musicians were built by magma that erupted preferably through preexisting fractures in the vicinity and parallel to the Murray FZ [*Lowrie et al.*, 1986; *Sager and Pringle*, 1987; *Pringle*, 1992]. This, however, is contradicted by two observations: (1) The formation of the VERs terminates at the Murray FZ and is not increasing as would be expected. Within the 130 km wide Murray FZ, several isolated volcanoes have erupted but do not show an obvious connection to the major faults carps, and (2) from satellite altimetry data it is obvious that the Pioneer FZ and the Murray FZ are almost perfect parallel over the northern Musicians province (lines A and B in Figure 3). Smaller fracture zones in the stress field between the large prominent fractures should follow this trend, and so should the Musicians VERs if they erupted along smaller fractures as proposed, e.g., by *Epp* [1984] and *Sager and Pringle* [1987]. However, as seen in Figure 3, the Musicians deviate by $\sim$8° from the general fracture zone trend between the Murray and Pioneer FZ. In the south, the emplacement of the ridges along preexisting fractures is also unlikely, even though the deviation of the Musicians trend from the overall direction of the fracture zones here is not as significant as in the north. While the fracture zone trend changes from south of the Murray FZ to north of it, as indicated by the extrapolated trend in Figure 3, this is not the case for the trend of the Musicians VERs, implying that the emplacement of the Musicians is not tied to the stresses of larger or smaller fracture zones in the area. However, the alignment of all Musicians ridges suggests their common evolution. A possible explanation is their emplacement above a narrow sublithospheric channel of melting asthenosphere from the Euterpe hot spot track to the Pacific-Farallon spreading center. As sublithospheric asthenosphere flow would tend to be driven by buoyancy, thus following the strongest gradient of lithospheric thickness, it would always tend to form perpendicular to the spreading center, possibly somewhat modified by the absolute plate motion. This is supported by the observation that the Musicians VERs are pointing toward a N-S oriented spreading center to the east of the Musicians province (Figure 3), which is coincident with the last observed magnetic anomaly after the Cretaceous ''quiet'' zone (M34 corresponding to 84 Ma in Figure 3) and is oriented in a N-S direction. This observation does not contradict the fact that the Musicians are not parallel to the major fracture zones, as these will not evolve perpendicular to the spreading center in a phase of oblique spreading. Oblique spreading is inferred from changes in spreading direction which are manifested in the splitting of the fracture zones into extensional relay zones of an en echelon staircase pattern observed for example along Mendocino FZ between 140°W and 165°W.

[23] The formation of en echelon ridge segments as observed along, e.g., the Italian Ridge (Figure 2) has been interpreted for other ridges to be caused by deformation processes resulting in tensional cracks [*Winterer and Sandwell*, 1987; *Geli et al.*, 1998; *Vlastelic et al.*, 1998]. However, in our interpretation the general 90° E-W trend of the Musician ridges is built by several volcanoes that have erupted through weakened lithosphere above an E-W striking sublithospheric melt channel. Plate stresses are involved in a later stage: By the weakening of the plate due to the magmatic activity and the additional stress induced by the gravitational load of the newly built volcanic edifices on the plate, these volcanoes act as an origin for the formation of linear cracks [*Kopp and Phipps Morgan*, 2000]. The common orientation of the en echelon ridge segments (trending $\sim$84°) depends on the crack orientation and thus on the direction of least compressional stress, i.e., on the regional stress field of the lithosphere. This stress field may be linked to processes such as shear stress near transform offsets of the spreading axis, ridge push, thermal contraction, or interaction between cracks. Hence a possible process to create the observed (WSW-ENE striking) en echelon segments superimposing the general E-W trend of the Musicians may be associated to cracks propagating away from volcanic centers in a regional stress field with tension vectors oblique to the spreading direction. The Musician en echelon ridge segments display descending elevations of the ends of the segments, which are centered around the largest volcanic edifice (indicated by water depth in Figures 2a and 2c). This central volcano may act as a nucleating flaw from where cracks propagate [*Kopp and Phipps Morgan*, 2000]. For the Pukapuka ridges it has been proposed that the presence of small conical or pancake-shaped volcanoes (which are also observed along the Italian and Bach Ridge, Figure 2) on the seafloor adjacent to mature ridges represent the first stage of volcanic activity leading to the development of linear ridge groups [*Lynch*, 2000]. This evolutionary sequence of events in ridge formation argues that the cracking is preceded by increased magmatic activity, which in the case of the Musicians would be related to the partially melting asthenospheric flow channel underneath a young and thin lithosphere.

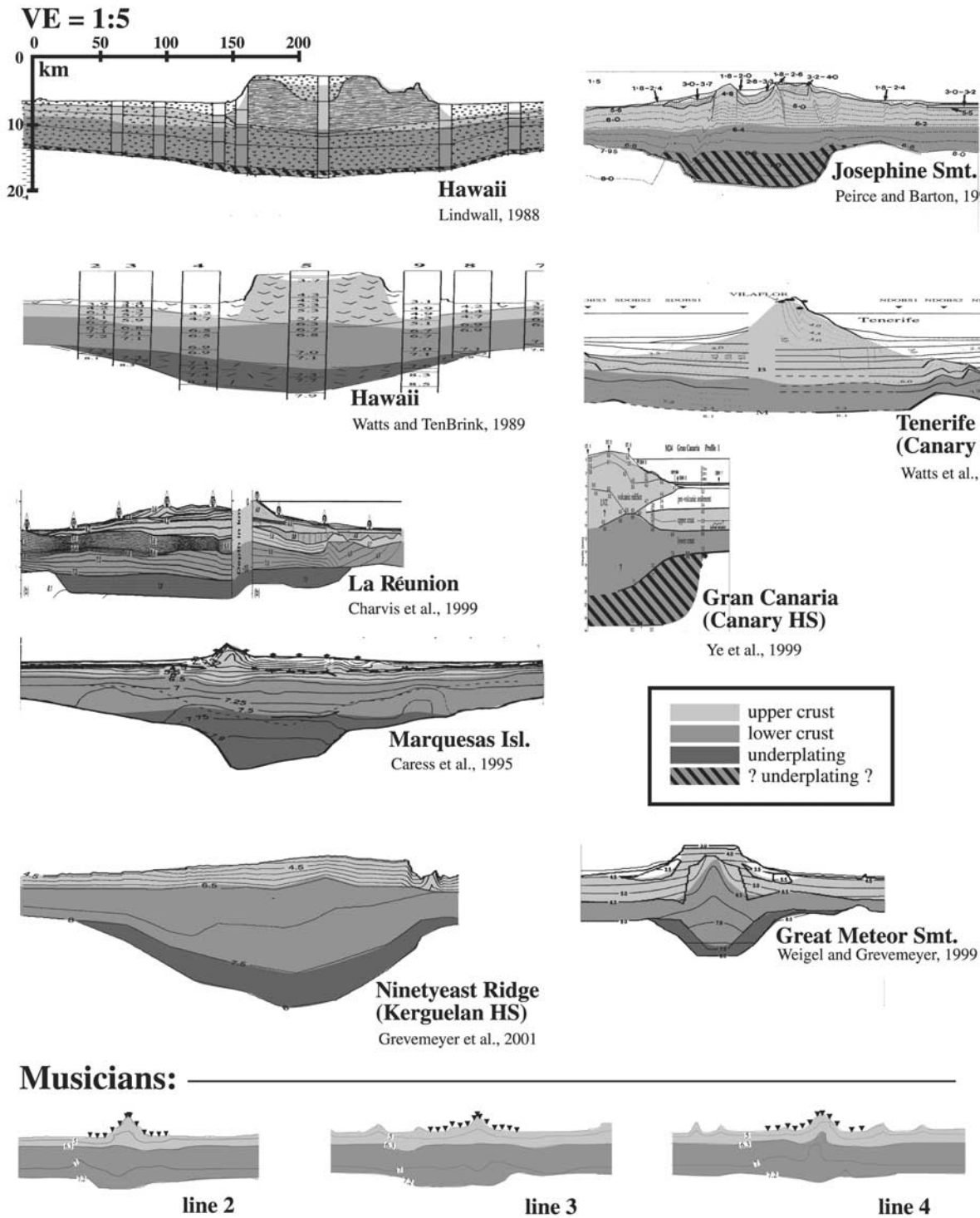

Figure 11. Global compilation of different hot spot related volcanic structures. All examples are scaled identically. Separation between upper and lower crust along all models is based only on velocities. Intrusive volcanism and underplating are characteristic for most of the volcanic provinces, which were located above a hot spot at the time of their formation. The Musicians are displayed at the bottom. They show much smaller dimensions and are dominated by extrusive volcanism. Their formation is linked to hot spot-ridge interaction, with them being between the Euterpe hot spot and the nearby Pacific-Farallon spreading center.

9. Crustal Age Constraints

[24] The magmatic feeding of spreading centers by neighboring mantle plumes over hundreds of kilometers has been suggested by a number of authors [*Vogt*, 1971; *Morgan*, 1978; *Epp*, 1984; *Schilling et al.*, 1985]. From the existence of at least two guyots in the study area (Figure 2), constraints on the distance of the Pacific Farallon spreading center to the Musicians ridges may be drawn. The flat top Rossini Seamount on the Italian Ridge lies in a water depth of 2.7 km (blowup in Figure 2). From the standard seafloor subsidence assuming 2500 m water depth at the spreading center (Parsons and Sclater, 1977), it is inferred that Rossini Seamount erupted on 1.7 Ma seafloor. Guyot 2 on Bach Ridge erupted on 0.2 Ma oceanic lithosphere. *Clague et al.* [2000] propose that flat top seamounts may also form without erosional influence from collapsing calderas, which are subsequently filled and subdued. However, the Vance, President Jackson or Taney seamounts shown by Clague display a strikingly different morphology compared to the Musicians, with an organized structure consisting of single volcanoes with ring-formed calderas lining up to an entire seamount chain. In contrast, the Musicians guyots have a much more irregular shape (e.g., Rossini Seamount in Figure 2) and all volcanoes are connected by diffuse ridge volcanism and do not form isolated structures. We believe that erosional processes in shallow water depths near the spreading axis built the Musicians flat tops.

[25] The digital magnetic isochron map of *Müller et al.* [1997] suggests a seafloor age of 107 Ma underneath Rossini Seamount near the western termination of Italian Ridge. An evolution of Rossini close to the spreading axis would thus imply that Rossini Seamount must be older than the oldest dredged samples from the Musicians province (maximum 96 Ma). As this is unlikely, we propose an alternative reconstruction of the seafloor underneath the Musicians formed during the Cretaceous quiet zone, which will explain the near-spreading axis location of the guyots at the time of their formation. The geometry of the Musicians offers an independent strong age constraint on the tectonic history of the Western Pacific: the reconstruction is based on the morphological geometry in the Musicians province, where the Euterpe hot spot trail ends abruptly in the north. The absence of a hot spot track north of the Mendocino FZ has been explained by the large offset across the fracture zone and the subduction of the Farallon plate [*Sager and Pringle*, 1987]. The oldest Musicians seamount is located just south of the Pioneer FZ with an Ar-Ar determined age of ~96 Ma implying that this is the time at which the hot spot crossed the Pioneer FZ. Prior to this time, Euterpe produced seamounts on the Farallon plate. The Pioneer FZ however displays a much shorter offset of ~200 km compared to Mendocino FZ. This is also evident from the surface traces of the fracture zones, where plate reorganizations result in large relay zones and a splitting of the fault from a single trace into a number of oblique subparallel tracks along Mendocino FZ, while "simple" kinks compensate the changes in plate motion along the short-offset Pioneer FZ. As prior to 96 Ma the Pacific-Farallon spreading center north of the Pioneer FZ must have been located westward of the hot spot track, while being placed eastward of the hot spot trail on the Pacific plate south of the Pioneer FZ, the hot spot must have crossed the Pioneer FZ in a small "window" determined by the ~200 km offset. Only this geographic setting explains the absence of the hot spot track north of the Pioneer FZ and its simultaneous presence today on the Pacific plate. This observation puts a geographic constraint on the location of the spreading center with regards to the hot spot track at 96 Ma. From this follows that the spreading center was located at a distance between 0 and 200 km east of the hot spot track. From the dating of magnetic anomalies [*Atwater and Severinghaus*, 1989] the first position of the spreading center after the Cretaceous quiet zone is known (M34 at 84 Ma). Interpolation then yields the approximate former positions of the spreading center in the Musicians province at the time of the VER emplacement (Figure 12).

[26] The observed guyots offer an additional second independent constraint on this reconstruction. Rossini Seamount, which was inferred to have been emplaced on 1.7 Ma crust, fits adequately to the new reconstruction, where it would be placed on ~2 Ma crust. Judging from the height of the second guyot, which is located toward the eastern end of Bach Ridge, it must have been created on 0.2 Ma crust. The reconstruction would place it on ~0.5 Ma crust. Thus for both flat tops a mean error of <0.5 Myr is inferred for the tectonic reconstruction.

10. Hot Spot-Ridge Interaction

[27] *Sager and Pringle* [1987] proposed a tectonic model for the formation of the Musicians, which involves a long section of Farallon plate that protruded into the Pacific plate. A change in spreading direction at ~90 Ma, as evidenced by the extensional relay zones along the neighboring fracture zones, induced the eruption of hot spot magma along fractures and cracks caused by the resulting tensional deformation. The corresponding change in the fracture zone trend to a staircase pattern has an approximate distance of 290 km to Rossini seamount. Assuming a spreading rate between 4.4 cm yr^{-1} [*Müller et al.*, 1997] and 7.4 cm yr^{-1} (this study) this implies that Rossini must have been built on 6.6 Ma or 3.7 Ma crust, respectively, which would have subsided too far for the flat top volcanoes to form and stands in contradiction to the 1.7 Ma computed from the depth of the eroded top. Another important aspect that cannot be explained by the model proposed by Sager and Pringle is the observation that the ridges terminate at the hot spot track. A model based on hot spot-ridge interaction best explains this geometry.

[28] On the basis of the newly acquired geophysical data presented here a possible evolution scenario for the Musicians VERs has been developed and is displayed in Figure 13. The Euterpe hot spot was close enough to the Pacific Farallon spreading center, that melting-asthenosphere could flow beneath the lithosphere to the spreading axis and feed it. The Euterpe mantle plume leaves a regular hot spot track on the Pacific plate. This track is the western limit of the VERs, which develop on top of a partially melting asthenospheric flow channel between the hot spot and the spreading center. Hot spot-ridge interaction has been shown to cause the development of aseismic ridges like Ninetyeast Ridge or Cocos Ridge by the production of thickened crust where hot

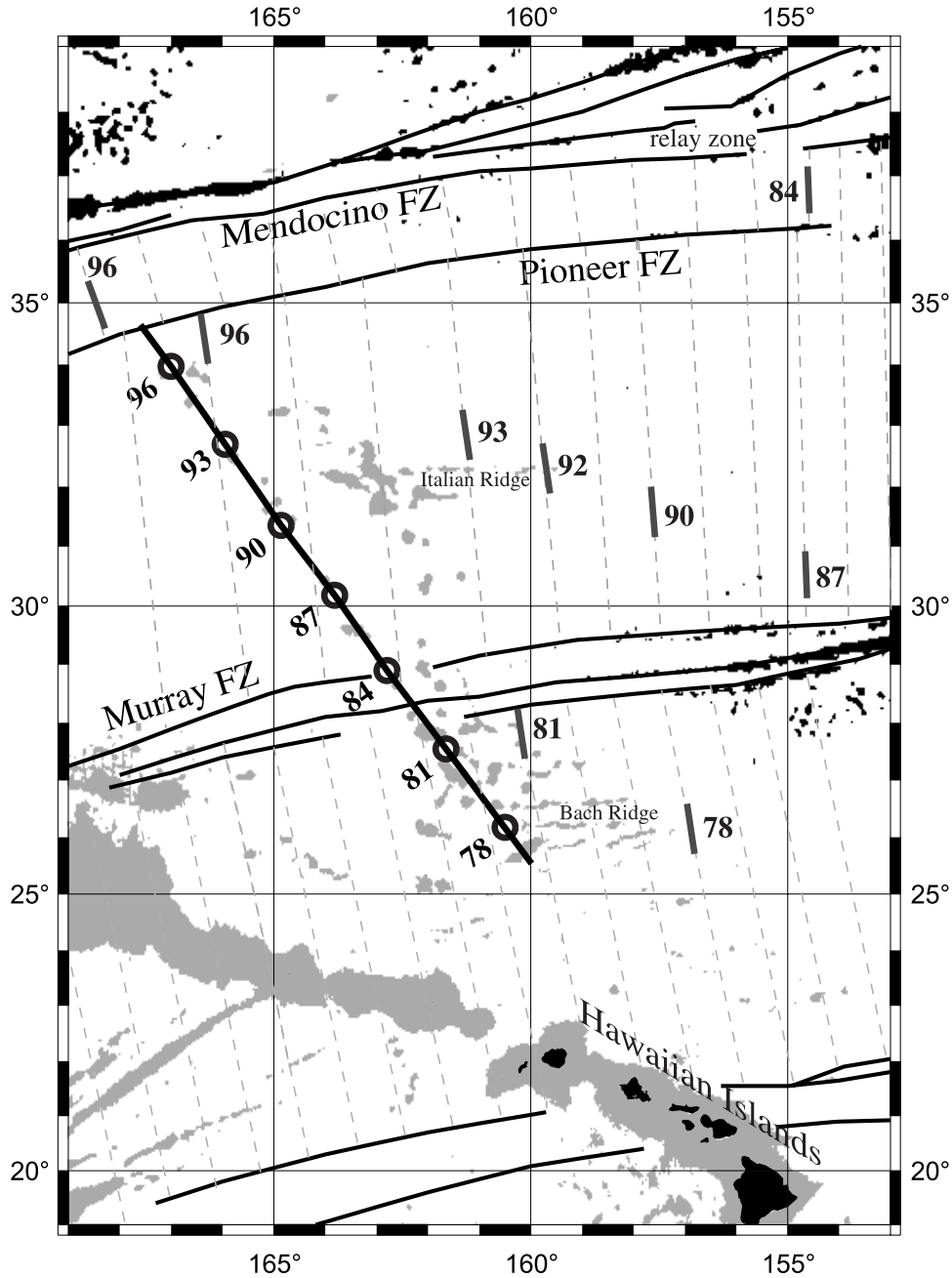

Figure 12. Proposed tectonic reconstruction based on geomorphological observations in the study area north of the Hawaiian seamount chain. The northwestward trending line is the track of the Cretaceous Euterpe hot spot with its age progression indicated in million years. The hot spot crossed the Pioneer fracture zone at ~97 Ma. Its track north of the FZ has been destroyed with the subduction of the Farallon plate. The former position of the Pacific-Farallon spreading center is indicated by the stippled lines and has been inferred from the crossing time of Euterpe over Pioneer FZ and from magnetic anomalies before the Cretaceous quiet zone. The position of guyots with respect to the spreading center yields a second, independent age constraint. The spreading center progressively moved away from Euterpe hot spot from north to south, until being shifted closer to the hot spot again by the offset across the Murray FZ. The Musicians VERs were formed between the hot spot and the spreading center, which explains their progressively increasing lengths and their westward termination at the hot spot track. When the distance between Euterpe and the spreading center grew too large at 93 Ma, formation of the VERs stopped but was reinitiated south of the Murray FZ.

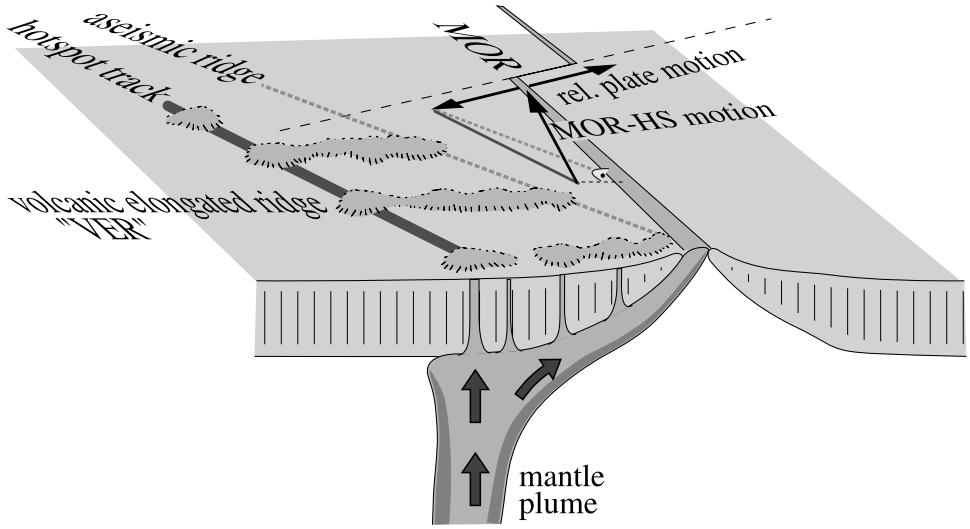

Figure 13. Formation of the Musicians VERs between the Euterpe hot spot and the Pacific-Farallon spreading center. When the hot spot was close enough to the ridge that melting-asthenosphere could be channeled beneath the lithosphere to the spreading axis and feed it, volcanic elongated ridges developed on top of the melting channel. Their orientation is perpendicular to the spreading center and thus differs from the azimuth of an aseismic ridge originating at the spreading center. The latter shows an orientation as indicated by the stippled line resulting from the sum of the relative plate motion and the motion of the hot spot (indicated by the dark hot spot track and the arrows at the spreading ridge.)

spot melt contributes to the production of crust at the spreading center. In principle, this mechanism may also apply for off-axis hot spots erecting an aseismic ridge as described by *Morgan* [1978] with a distinct azimuth which equals the sum of the absolute plate motion over the hot spot and the relative plate motion along the spreading direction. However, in this scenario an aseismic ridge would have an orientation as indicated by the stippled line in Figure 13, which significantly differs from the trend of the observed VERs. The location and geometry of the Musicians ridges rather imply that they were constructed off axis on top of the melting-asthenosphere channel, the shortest path between hot spot and spreading center and perpendicular to the spreading axis, as discussed above. The eastern termination of the VERs is then given by the former position of the spreading axis at the time of the volcanic ridge emplacement (Figure 12). Between 96 Ma and 84 Ma, the distance between hot spot and spreading center progressively increased as the spreading center migrated eastward from the hot spot, resulting in progressive lengthening of each VER. Formation of VERs ceased south of Italian Ridge at 91 Ma. Several scenarios are possible: (1) the distance between the hot spot and the spreading center grew too large for off axis magmatism to develop south of Italian Ridge, (2) failure in melt generation occurred near the hot spot and propagated toward the ridge, or (3) maybe the channel broadened with distance from the hot spot, resulting in too little melt to break through the lithosphere. All these scenarios imply an evolution of the Musicians VERs by interaction of the Euterpe hot spot and the Pacific-Farallon spreading center which explains the observation that ridge formation is reinitiated south of the Murray FZ: after the Murray FZ migrated over the hot spot at 81 Ma, the spreading center was again close enough to the hot spot for VERs to form between them (Figure 12). As expected here, the VERs again show increasing lengths to the south.

11. Discussion

[29] Not only in the case of the Musicians has it been observed that aseismic ridges in the vicinity of spreading centers resulting from hot spot-ridge interaction often do not follow the azimuth predicted by *Morgan* [1978], though plume-ridge interaction seems to play a major role in their evolution [*Morgan*, 1978; *Schilling*, 1985; *Small*, 1995]. Numerical models by *Ito et al.* [1997] infer a maximum possible distance of plume-ridge interaction, which scales with plume source volume flux and ridge spreading rate, implying that there is an upper limit to the hot spot-spreading center separation as we suggest for the Musicians. The plume affects the ridge in a number of ways: the geochemical signature shows signs of plume enrichment (as reported for e. g. lead isotope ratios [*Kingsley and Schilling*, 1998]) and could additionally affect the topography and crustal thickness in the vicinity of the ridge [*Maia et al.*, 2000]. This also depends on the effectiveness of the melt channeling as there seems to be a difference in the amounts of plume material reaching the ridge axis for different ridge-hot spot systems [*Maia et al.*, 2000]. The area over which the ridge is affected by the plume is 125–200% as broad as the maximum plume ridge separation, so that the excess plume melt is distributed over a large segment of the ridge and possibly does not cause changes in topography or crustal thickness [*Ito et al.*, 1997]. We propose that this scenario applies to the Musicians. The VERs are terminated to the east at the assumed former position of the spreading axis where the excess melt is

distributed along axis. This explains why no ''Morgan-type'' aseismic ridges following the predicted azimuth (stippled line in Figure 13) are observed here.

[30] For the western Easter Salas y Gomez seamount chain focused flow along an ~70 km wide channel toward the EPR has been proposed by *Kingsley and Schilling* [1998]. Their Pb isotope investigations are not compatible with a passive radial melt mixing here. The observation of a neovolcanic gap close to the EPR may be associated with counter flow away from the EPR or by a capturing and focusing of the plume material by the upwelling system of the ridge [*Kingsley and Schilling*, 1998]. As the former position of the Pacific Farallon plate with regards to the Musicians VERs may be inferred from the formation depths of the guyots in the study area, a similar volcanic gap in the Musicians province is unlikely, implying that the maximum length of the VERs may better correspond to a maximum hot spot-ridge interaction distance as proposed by *Ito et al.* [1997].

12. Conclusions and Relation to Other Aseismic Ridge Groups

[31] The Musicians volcanic elongated ridges were formed by plume-hot spot interaction on top of sublithospheric partially melting asthenospheric channels between the Euterpe hot spot and its neighboring Pacific-Farallon spreading center. This model is supported by the geometry, ages, and bathymetry of the investigated volcanoes. The Musicians volcanoes form coherent volcanic ridges, which show a mostly extrusive style of volcanism as inferred from the tomographic investigations of the newly acquired seismic data presented here. Crustal thickening is recognized in oceanic layer 2 rather than in layer 3. Although reduced seismic velocities in the upper mantle were recorded here, these could not be associated with underplating. The extrusive mode of formation stands in contrast to the seismic structure of many aseismic ridges, where crustal thickening is mostly accommodated by intrusive underplating of high-velocity lower crust. The progressively increasing lengths of the Musicians VERs from north to south are a distinct feature of this volcanic province. From this morphological geometry a maximum hot spot spreading center separation of ~400 km, over which sublithospheric plume-ridge interaction occurred, is observed. Another important aspect of this study is the recognition of two independent age constraints for the Pacific crust during the Cretaceous quiet zone. From the existence of guyots in the Musicians province the former location of the Farallon-Pacific spreading center may be inferred. Its position at 96 Ma just south of the Pioneer FZ may additionally be derived from the unique geometrical setting here, which yields a window of maximum 200 km width for Euterpe hot spot to pass from underneath Farallon plate, where its track east of the spreading center was ultimately destroyed, to the Pacific plate, where it was located west of the ridge. Assuming that the Musicians VERs developed in conjunction with Euterpe hot spot, as is highly likely due to the western termination of the ridges at the hot spot track, a tectonic reconstruction of this area of the Pacific during the Cretaceous quiet zone has been developed which differs by up to 10 Myr from the isochron age map by *Müller et al.* [1997].

[32] The proposed formation scenario may be applicable to a number of aseismic ridges observed near spreading centers. Along the Eastern termination of the Foundation Chain, which approaches the PAR, a change in fabric from the isolated seamounts caused by the passing of the Pacific plate over the Foundation plume to a broad region of elongated, en echelon ridges similar to the Musicians VERs is observed [*O'Connor et al.*, 1998; *Maia et al.*, 2000]. The Tuamotu Isles east of Tahiti form the subaerial trace of en echelon ridges, which may represent fossil VERs in the Central Pacific [*Searle et al.*, 1995]. Another example for a volcanic ridge formed on top of a sublithospheric plume flux is the western Easter-Salas y Gomez seamount chain as proposed by *Kingsley and Schilling* [1998], where none of the seamounts are associated with any of the apparent fracture zones, similar to the geometry of the Musicians VERs.

[33] **Acknowledgments.** We thank all participants of the HULA cruise and especially Capt. Andresen and his crew for their professional work at sea. The HULA project is supported by the German Federal Ministry for Science and Technology (BMBF). We would also like to thank Marcia Maia, an anonymous reviewer, the Associate Editor, and Editor Francis Albarede for careful reviews of the manuscript.

References

Atwater, T., and J. Severinghaus, Tectonic maps of the northeast Pacific, in *The Geology of North America*, vol. N, *The Eastern Pacific Ocean and Hawaii*, edited by E. L. Winterer, D. M. Hussong, and R. W. Decker, pp. 15–20, Geol. Soc. of Am., Boulder, Colo., 1989.

Bialas, J., N. Kukowski, and Shipboard Science Party, GEOPECO (SONNE Cruise SO-146): Geophysical Experiments at the Peruvian continental margin, cruise report, Geomar, Kiel, Germany, 2000.

Binard, N., P. Stoffers, R. Hekinian, and R. C. Searle, Intraplate en echelon volcanic ridges in the South Pacific west of the Easter microplate, *Tectonophysics*, *263*, 23–37, 1996.

Caress, D. W., and D. N. Chayes, Improved processing of Hydrosweep DS multibeam data on the R/V *Maurice Ewing*, *Mar. Geophys. Res.*, *18*, 631–650, 1996.

Clague, D. A., J. R. Reynolds, and A. S. Davis, Near-ridge seamount chains in the northeastern Pacific Ocean, *J. Geophys. Res.*, *105*, 16,541–16,561, 2000.

Epp, D., Age and tectonic relationships among volcanic chains on the Pacific plate, Ph.D. thesis, 199 pp., Univ. of Hawaii, Honolulu, 1978.

Epp, D., Possible perturbations to hotspot traces and implications for the origin and structure of the Line Islands, *J. Geophys. Res.*, *89*, 11,273–11,286, 1984.

Flueh, E. R., J. O'Connor, J. Phipps Morgan, J. Wagner, and Shipboard Science Party, HULA (SONNE Cruise SO-142): Interdisciplinary investigations on the timing of the Hawaii-Emperor Bend and the origin of lithospheric anomalies along the Musician seamount chain, cruise report, Geomar, Kiel, Germany, 1999.

Flueh, E. R., J. Bialas, P. Charvis, and Shipboard Science Party, SALIERI (SONNE Cruise SO-159): South American Lithospheric Transects Across Volcanic Ridges, cruise report, Geomar, Kiel, Germany, 2001.

Freedman, A. P., and B. Parsons, Seasat-derived gravity over the Musicians Seamounts, *J. Geophys. Res.*, *91*, 8325–8340, 1986.

Geli, L., D. Aslanian, J.-L. Olivet, I. Vlastelic, L. Dosso, H. Guillou, and H. Bougault, Location of Louisville hotspot and origin of Hollister Ridge: Geophysical constraints, *Earth Planet. Sci. Lett.*, *164*, 31–40, 1998.

Grant, J. A., and R. Schreiber, Modern swath sounding and subbottom profiling technology for research applications: The Atlas Hydrosweep and Parasound systems, *Mar. Geophys. Res.*, *12*, 9–19, 1990.

Grevemeyer, I., E. R. Flueh, C. Reichert, J. Bialas, D. Klaeschen, and C. Kopp, Crustal architecture and deep structure of the Ninetyeast Ridge hotspot trail from active-source ocean bottom seismology, *Geophys. J. Int.*, *144*, 1–22, 2001.

Hanan, B. B., R. H. Kingsley, and J.-G. Schilling, Migrating ridge-hotspot interactions: Pb isotope evidence in the South Atlantic, *Nature*, *322*, 137–144, 1986.

Hey, R. N., and P. R. Vogt, Spreading center jumps and sub-axial asthenosphere flow near the Galapagos hotspot, *Tectonophysics*, *37*, 41–52, 1977.

Hole, J. A., and B. C. Zelt, 3-D finite-difference reflection travel times, *Geophys. J. Int.*, *121*, 427–434, 1995.

Ito, G., J. Lin, and C. W. Gable, Interaction of mantle plumes and migrating mid-ocean ridges: Implications for the Galapagos plume-ridge system, *J. Geophys. Res.*, *102*, 15,403–15,417, 1997.

Johnson, G. L., and P. R. Vogt, Mid-Atlantic Ridge from 46°N to 51°N, *Geol. Soc. Am. Bull.*, *84*, 3443–3462, 1973.

Keller, R. A., R. A. Duncan, and M. R. Fisk, Geochemistry and $^{40}Ar/^{39}Ar$ geochronology of basalts from ODP Leg 145 (North Pacific Transect, *Proc. Ocean Drill. Program Sci. Results*, *145*, 333–344, 1995.

Keller, R. A., M. R. Fisk, and W. M. White, Isotopic evidence for late cretaceous plume-ridge interaction at the Hawaiian hotspot, *Nature*, *405*, 673–676, 2000.

Kingsley, R. H., and J.-G. Schilling, Plume-ridge interaction in the Easter-Salas y Gomez seamount chain-Easter Microplate system: Pb isotope evidence, *J. Geophys. Res.*, *103*, 24,159–24,177, 1998.

Kissling, E., W. L. Ellsworth, D. Eberhart-Phillips, and U. Kradolfer, Initial reference models in local earthquake tomography, *J. Geophys. Res.*, *99*, 19,635–19,646, 1994.

Kopp, C., and J. Phipps Morgan, Is the en-echelon formation of volcanic elongated ridges due to interacting "dike-like" magma propagation away from discrete volcanic centers?, Eos Trans, *Eos Trans. AGU*, *81*(48), Fall Meet. Suppl., Abstract V21F-11, 2000.

Lindwall, D., A two-dimensional seismic investigation of crustal structure under the Hawaiian Islands near Oahu and Kauai, *J. Geophys. Res.*, *94*, 12,107–12,122, 1988.

Lonsdale, P., and K. D. Klitgord, Structure and tectonic history of the eastern Panama Basin, *Geol. Soc. Am. Bull.*, *89*, 981–999, 1978.

Lowrie, A., C. Smoot, and R. Batiza, Are oceanic fracture zones locked and strong or weak?: New evidence for volcanic activity and weakness, *Geology*, *14*, 242–245, 1986.

Lynch, M. A., Linear ridge groups: Evidence for tensional cracking in the Pacific Plate, *J. Geophys. Res.*, *104*, 29,321–29,333, 2000.

Mahoney, J. J., J. D. Macdougall, G. W. Lugmair, and K. Gopalan, Kerguelen hot spot source for Rajmahal Traps and Ninety-east Ridge?, *Nature*, *303*, 385–389, 1983.

Maia, M., and J. Arkani-Hamed, The support mechanism of the young Foundation Seamounts inferred from bathymetry and gravity, *Geophys. J. Int.*, *149*, 190–210, 2002.

Maia, M., et al., The Pacific-Antarctic Ridge-Foundation hotspot interaction: A case study of a ridge approaching a hotspot, *Mar. Geol.*, *167*, 61–84, 2000.

Morgan, W. J., Rodriguez, Darwin, Amsterdam,. . ., A second type of Hotspot Island, *J. Geophys. Res.*, *83*, 5355–5360, 1978.

Müller, D., W. R. Roest, J. Y. Royer, L. M. Gahagan, and J. G. Sclater, Digital isochrons of the world's ocean floor, *J. Geophys. Res.*, *102*, 3211–3214, 1997.

O'Connor, J. M., P. Stoffers, and J. R. Wijbrans, Migration rate of volcanism along the Foundation Chain, SE Pacific, *Earth Planet. Sci. Lett.*, *164*, 41–59, 1998.

Peirce, C., and P. J. Barton, Crustal structure of the Madeira-Tore Rise, eastern North Atlantic—Results of a DOBS wide-angle and normal incidence seismic experiment in the Josephine Seamount region, *Geophys. J. Int.*, *106*, 357–378, 1991.

Pringle, M. S., Geochronology and Petrology of the Musicians Seamounts, and the search for hot spot volcanism in the Cretaceous Pacific, Ph.D. thesis, Univ. of Hawaii, Honolulu, 1992.

Pringle, M. S., Age progressive volcanism in the Musicians seamounts: A test of the hot spot hypothesis for the late Cretaceous Pacific, in *The Mesozoic Pacific: Geology, Tectonics, and Volcanism*, *Geophys. Monogr. Ser.*, vol. 77, edited by M. S. Pringle et al., pp. 187–215, AGU, Washington, D. C., 1993.

Sager, W. W., and M. S. Pringle, Paleomagnetic constraints on the origin and evolution of the Musicians and South Hawaiian Seamounts, central Pacific Ocean, in *Seamounts, Islands, and Atolls*, *Geophys. Monogr. Ser.*, vol. 43, edited by B. H. Keating et al., pp. 133–162, AGU, Washington, D. C., 1987.

Sandwell, D., and W. H. F. Smith, Global marine gravity from Geosat and ERS-1 satellite altimetry, *J. Geophys. Res.*, *102*, 10,039–10,054, 1997.

Sandwell, D. T., E. L. Winterer, J. Mammerickx, R. A. Duncan, M. A. Lynch, D. A. Levitt, and C. A. Johnson, Evidence for diffuse extension of the Pacific Plate from Puka-Puka ridges and Cross-grain gravity lineations, *J. Geophys. Res.*, *100*, 15,087–15,099, 1995.

Schilling, J.-G., Upper mantle heterogeneities and dynamics, *Nature*, *314*, 62–67, 1985.

Schilling, J.-G., G. Thompson, R. Kingsley, and S. Humphris, Hotspot-migrating ridge interaction in the South Atlantic, *Nature*, *313*, 187–191, 1985.

Schouten, H., H. J. B. Dick, and K. D. Klitgord, Migration of mid-ocean-ridge volcanic segments, *Nature*, *326*, 835–839, 1987.

Searle, R. C., J. Francheteau, and B. Cornaglia, New observations on mid-plate volcanism and the tectonic history of the Pacific plate, Tahiti to Easter microplate, *Earth Planet. Sci. Lett.*, *131*, 395–421, 1995.

Sempere, J.-C., and J. R. Cochran, The Southwest Indian Ridge between 88°E and 118°E: Variations in crustal accretion at constant spreading rate, *J. Geophys. Res.*, *102*, 15,489–15,506, 1997.

Small, C., Observations of ridge-hotspot interactions in the Southern Ocean, *J. Geophys. Res.*, *100*, 17,931–17,946, 1995.

Staples, R., R. White, B. Brandsdottir, W. Menke, P. Maguire, and J. McBride, Faroes-Iceland Experiment, 1, The crustal structure of northeastern Iceland, *J. Geophys. Res.*, *102*, 7849–7866, 1997.

Verma, S. P., J.-G. Schilling, and D. G. Waggoner, Neodymium isotopic evidence for Galapagos hotspot-spreading centre system evolution, *Nature*, *306*, 654–657, 1983.

Vlastelic, I., L. Dosso, H. Guillou, H. Bougault, L. Geli, J. Etoubleau, and J. L. Joron, Geochemistry of the Hollister Ridge: Relation with the Louisville hotspot and the Pacific-Antarctic Ridge, *Earth Planet. Sci. Lett.*, *160*, 777–793, 1998.

Vogt, P. R., Asthenosphere motion recorded by the ocean floor south of Iceland, *Earth Planet. Sci. Lett.*, *13*, 153–160, 1971.

Walther, C. H. E., The crustal structure of the Cocos Ridge off Costa Rica, *J. Geophys. Res.*, *108*, doi:10.1029/2001JB000888, in press, 2003.

Watts, A. B., and U. S. ten Brink, Crustal structure, flexure, and subsidence history of the Hawaiian Islands, *J. Geophys. Res.*, *94*, 10,473–10,500, 1989.

Watts, A. B., C. Peirce, J. Collier, R. Dalwood, J.-P. Canales, and T. J. Henstock, A seismic study of lithospheric flexure at Tenerife, Canary Islands, *Earth Planet. Sci. Lett.*, *146*, 431–448, 1997.

Weigel, W., and I. Grevemeyer, The Great Meteor seamount: Seismic structure of a submerged intraplate volcano, *J. Geodyn.*, *28*, 27–40, 1999.

Wessel, P., and W. H. F. Smith, Free software helps map and display data, *Eos Trans. AGU*, *72*, 445–446, 1991.

Winterer, E. L., and D. T. Sandwell, Evidence from en-echelon Cross-grain ridges for tensional cracks in the Pacific Plate, *Nature*, *329*, 534–535, 1987.

Ye, S., J. P. Canales, R. Rihm, J. J. Danobeitia, and J. Gallart, A crustal transect through the northern and northeastern part of the volcanic edifice of Gran Canaria, Canary Islands, *J. Geodyn.*, *28*, 3–26, 1999.

Yu, D., D. Fontignie, and J.-G. Schilling, Mantle plume-ridge interactions in the central North Atlantic: A Nd isotope study of Mid-Atlantic Ridge basalts from 30N to 50N, *Earth Planet. Sci. Lett.*, *146*, 259–272, 1997.

Zelt, C. A., and P. J. Barton, Three-dimensional seismic refraction tomography: A comparison of two methods applied to data from the Faeroe Basin, *J. Geophys. Res.*, *103*, 7187–7210, 1998.

Zelt, C. A., and R. B. Smith, Seismic travel time inversion for 2-D crustal velocity structure, *Geophys. J. Int.*, *108*, 16–34, 1992.

E. R. Flueh, C. Kopp, H. Kopp, J. Phipps Morgan, and W. Weinrebe, GEOMAR Research Center for Marine Geosciences, Wischhofstr. 1-3, 24148 Kiel, Germany. (eflueh@geomar.de; ckopp@geomar.de; hkopp@geomar.de; jmorgan@geomar.de; wweinrebe@geomar.de)

W. J. Morgan, Department of Geosciences, Guyot Hall, Princeton University, Princeton, NJ 08544-1003, USA. (wjmorgan@princeton.edu)